

Accepted Manuscript

Design, synthesis and biological evaluation of novel 7-amino-[1,2,4]triazolo[4,3-*f*]pteridinone, and 7-aminotetrazolo[1,5-*f*]pteridinone derivative as potent antitumor agents

Yunlei Hou, Liangyu Zhu, Zhiwei Li, Qi Shen, Qiaoling Xu, Wei Li, Yajing Liu, Ping Gong

PII: S0223-5234(18)31046-8

DOI: <https://doi.org/10.1016/j.ejmech.2018.12.009>

Reference: EJMECH 10942

To appear in: *European Journal of Medicinal Chemistry*

Received Date: 17 September 2018

Revised Date: 1 December 2018

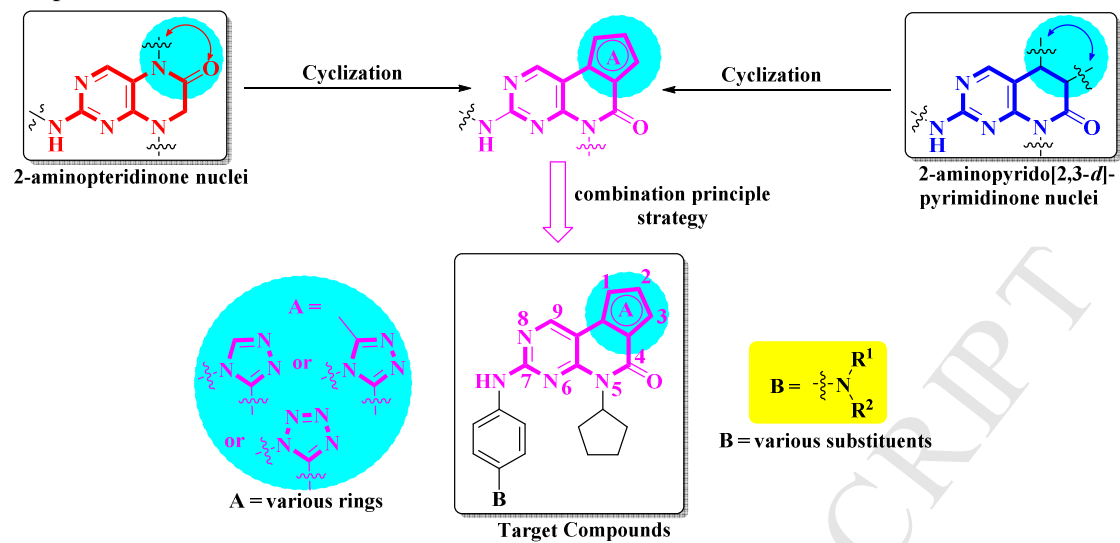
Accepted Date: 3 December 2018

Please cite this article as: Y. Hou, L. Zhu, Z. Li, Q. Shen, Q. Xu, W. Li, Y. Liu, P. Gong, Design, synthesis and biological evaluation of novel 7-amino-[1,2,4]triazolo[4,3-*f*]pteridinone, and 7-aminotetrazolo[1,5-*f*]pteridinone derivative as potent antitumor agents, *European Journal of Medicinal Chemistry* (2019), doi: <https://doi.org/10.1016/j.ejmech.2018.12.009>.

This is a PDF file of an unedited manuscript that has been accepted for publication. As a service to our customers we are providing this early version of the manuscript. The manuscript will undergo copyediting, typesetting, and review of the resulting proof before it is published in its final form. Please note that during the production process errors may be discovered which could affect the content, and all legal disclaimers that apply to the journal pertain.



Graphical abstract



Two series of novel 7-amino-[1,2,4]triazolo[4,3-*f*]pteridinone, and 7-aminotetrazolo[1,5-*f*]pteridinone derivatives were designed, synthesized and evaluated for their biological activity.

Design, synthesis and biological evaluation of novel 7-amino-[1,2,4]triazolo[4,3-f]pteridinone, and 7-aminotetrazolo[1,5-f]pteridinone derivative as potent antitumor agents

Yunlei Hou, Liangyu Zhu, Zhiwei Li, Qi Shen, Qiaoling Xu, Wei Li, Yajing Liu*, Ping Gong*

*Key Laboratory of Structure-Based Drug Design and Discovery, Ministry of Education, Shenyang Pharmaceutical University, 103 Wenhua Road, Shenhe District, Shenyang, 110016, China.***Abstract**

To develop novel therapeutic agents with anticancer activities, two series of novel 7-amino-[1,2,4]triazolo[4,3-f]pteridinone, and 7-aminotetrazolo[1,5-f]pteridinone derivatives were designed and synthesized. All compounds were tested for anti-proliferative activities against five cancer cell lines. The structure-activity relationships (SARs) studies were conducted through the variation in two regions, the moiety of **A** ring and the terminal aniline **B** on pteridinone core. 1-Methyl-1,2,4-triazole derivative **L**₇ with 2,6-dimethylpiperazine showed the most potent antiproliferative activity against A549, PC-3, HCT116, MCF-7 and MDA-MB-231 cell lines with IC₅₀ values of 0.16 μM, 0.30 μM, 0.51 μM, 0.30 μM, and 0.70 μM, respectively. Combined with the results of the molecular docking and enzymatic studies, the PLK1 was very likely to be one of the drug targets of compound **L**₇. Furthermore, to clarify the anticancer mechanism of compound **L**₇, further explorations in the bioactivity were conducted. The results showed that compound **L**₇ obviously inhibited proliferation of A549 cell lines, induced a great decrease in mitochondrial membrane potential leading to apoptosis of cancer cells, suppressed the migration of tumor cells, and arrested G1 phase of A549 cells.

1. Introduction

Despite continued research efforts, cancer remains the second leading disease after cardiovascular and one of the major public health problems characterized by uncontrolled growth and spread of the abnormal cells [1]. The Global Burden of Disease (GBD) 2015 studies stated that the most common types of cancer are breast, colorectal, and lung cancer in females and prostate, colorectal, and lung cancer in males [2-3]. To combat with cancer, lots of efforts have been concentrated on the design and synthesis of new antitumor drugs with low toxicity and high efficiency to normal cells and tissues. For these purposes, combination principle strategy has been extensively employed to develop new antineoplastic drugs that acted synergistic on multiple targets, *via* fusing two/more active pharmacophores covalently in a single-hybrid molecule with dual/multiple anticancer activity [4].

Recently, accumulating evidences have illustrated that heterocyclic scaffolds are important tool in the search for new active substances with a lot of potential applications [5]. Particularly, substituted 2-aminopteridinone skeleton has been described as a privileged structure, which appears extensively in many unrelated areas of biology and medicine. Especially, it could inhibit several cancer related enzymes as well as modulate the activity of many receptors. For example, PLK1 inhibitor **I** (currently in phase III clinical trials at Boehringer Ingelheim for the treatment of acute myeloid leukemia), EGFR inhibitor **II**, beta-amyloid (Abeta) production inhibitor **III**, and ALK inhibitor **IV**, *et al.* (**Fig. 1**) [6-9]. These characteristics indicated that the extent of ongoing interests toward new 2-aminopteridinone derivatives and prompted us to develop this pharmacophore as novel promising drugs.

*Corresponding author. E-mail address: gongpinggp@126.com (P. Gong). lyjpharm@126.com (Y.J. Liu).

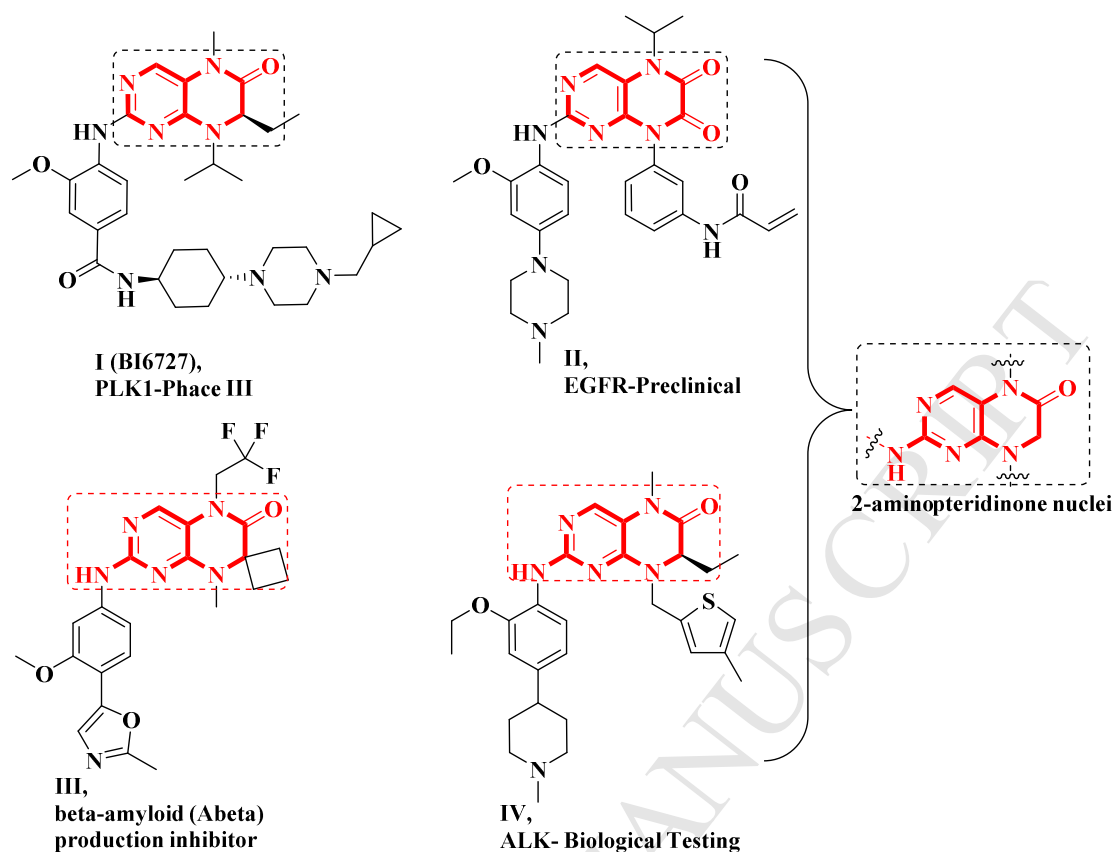


Fig. 1. Structures of representative kinase inhibitors containing 2-aminopyridinone nuclei.

In recent years, 2-aminopyrido[2,3-*d*]pyrimidinone derivatives have received considerable attention in anticancer agents due to their admirable inhibitory activity against CDK4/6 kinases, FGFR kinases, PI3K kinases, and MAPK kinases, which play critical roles in the regulation of tumor genesis [10-13]. Among these derivatives (**Fig. 2**), palbociclib (**V**), the first orally bioavailable CDK4/6 kinase inhibitor, was approved by FDA for the treatment of hormone-receptor positive breast cancer in February 2015. The co-crystal structure of palbociclib in complex with CDK6 kinase domains (PDB code: 5L2I) revealed that the 2-aminopyrido[2,3-*d*]pyrimidinone framework played key roles in the interaction with CDK6 kinase due to their binding modes and the presence of hydrogen bonds [14]. Thus, the development of such small molecules with 2-aminopyrido[2,3-*d*]pyrimidinone framework, which can readily bind with various enzymes and receptors through hydrogen bonds, is an effectual process to develop new antineoplastic drugs.

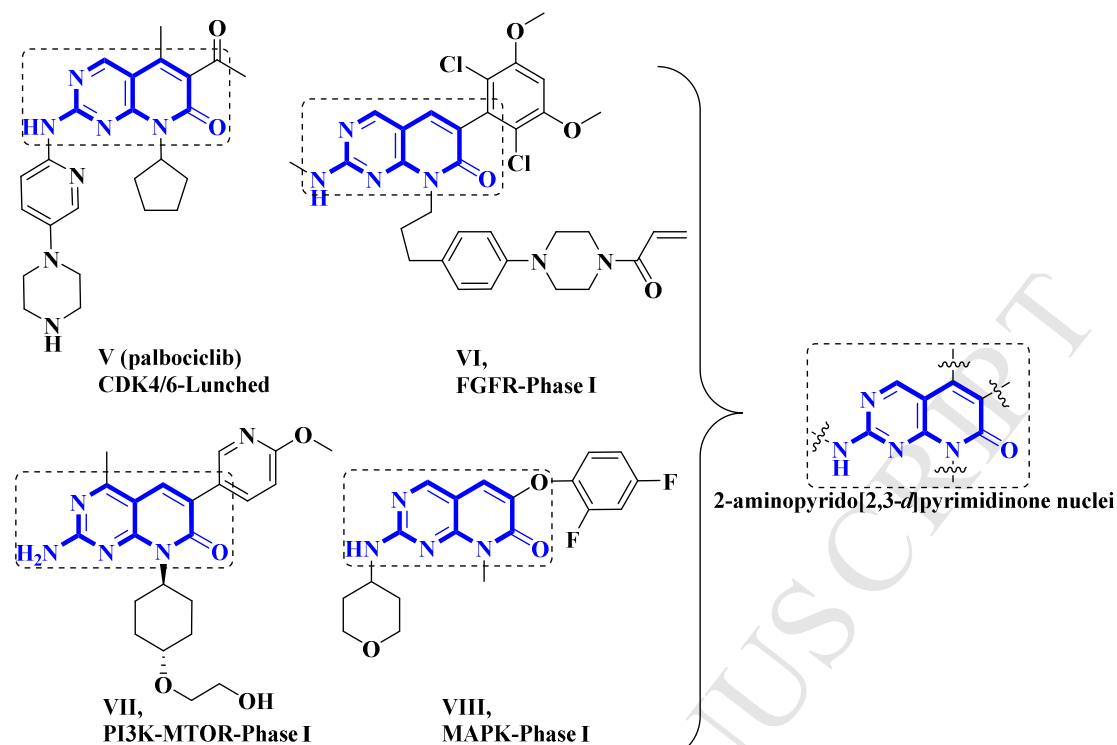


Fig. 2. Structures of representative kinase inhibitors containing 2-aminopyrido[2,3-*d*]pyrimidinone nuclei.

In addition, triazolo and tetrazolo heterocycles constitute a very important class of heterocyclic compounds in the area of drug design, which exhibit a broad spectrum of biological activity, including anti-inflammatory [15], central nervous system (CNS) dispersant [16], antimicrobial [17], anti-AIDS [18], antifertility [19], anticancer [20], and anticonvulsant [21]. As continue of our effort to discover new types of antitumor lead compounds and our interest in studying the influence of fusing triazolo or tetrazolo to the 2-aminopteridinone or 2-aminopyrido[2,3-*d*]pyrimidinone frameworks, so these combined substructures could exhibit synchronous antitumor effect. (**Fig. 3**) Furthermore, the hydrophilic “tail” piperidine motif exposing to the solvent has been investigated extensively in recent years [22-24], indicating that modification on the “tail” (**B**) could be tolerant to maintain efficacies.

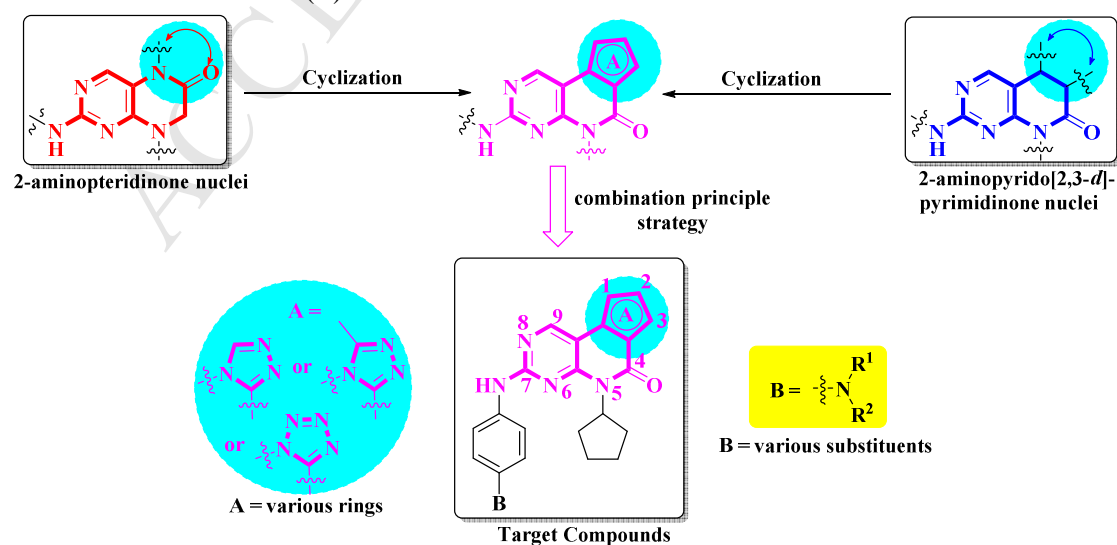


Fig. 3. Design strategy for the target compounds.

Murray et al. [14] and Adolf et al. [25] reported that the 2-aminopyrido[2,3-*d*]pyrimidinone moiety of palbociclib and 2-aminopteridinone moiety of BI6727 were combined within the CDK6 and PLK1 active site, respectively. And the side chain anilines moiety were combined within solvent region. Meanwhile, compound **H**₂, **Y**₂, **L**₂ contained similar structural feature with palbociclib and BI6727 including hydrophilic aniline side chain and pteridinone or pyrido[2,3-*d*]pyrimidinone fragments. So in order to better understand the anti-tumor mechanisms, molecular docking models of **H**₂, **Y**₂, **L**₂ were performed based upon the cocrystal structure of CDK6 with palbociclib (PDB code: 5L2I) and PLK1 with BI6727 (PDB code: 3FC2). As shown in **Fig. 4**, compound **H**₂, **Y**₂, **L**₂ occupied the kinase domain in a similar manner to palbociclib and BI6727. Combined with the results of docking analysis, CDK6 or PLK1 was very likely to be one of the potential drug targets of these 7-amino-pteridinone derivatives.

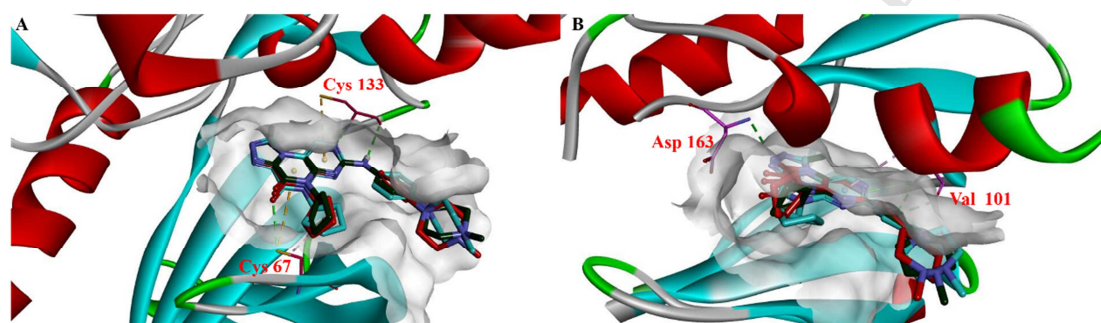


Fig. 4. (A) The predicted binding models of **H**₂ (blue sticks), **Y**₂ (red sticks), **L**₂ (green sticks) with PLK1 (PDB code: 3FC2); (B) The binding models of **H**₂ (blue sticks), **Y**₂ (red sticks), **L**₂ (green sticks) with CDK6 (PDB code: 5L2I).

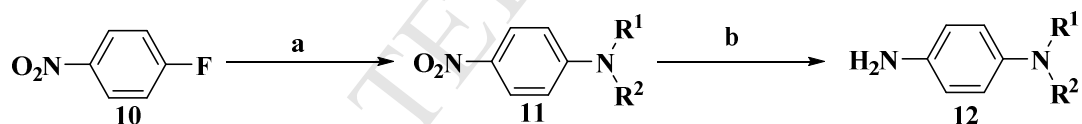
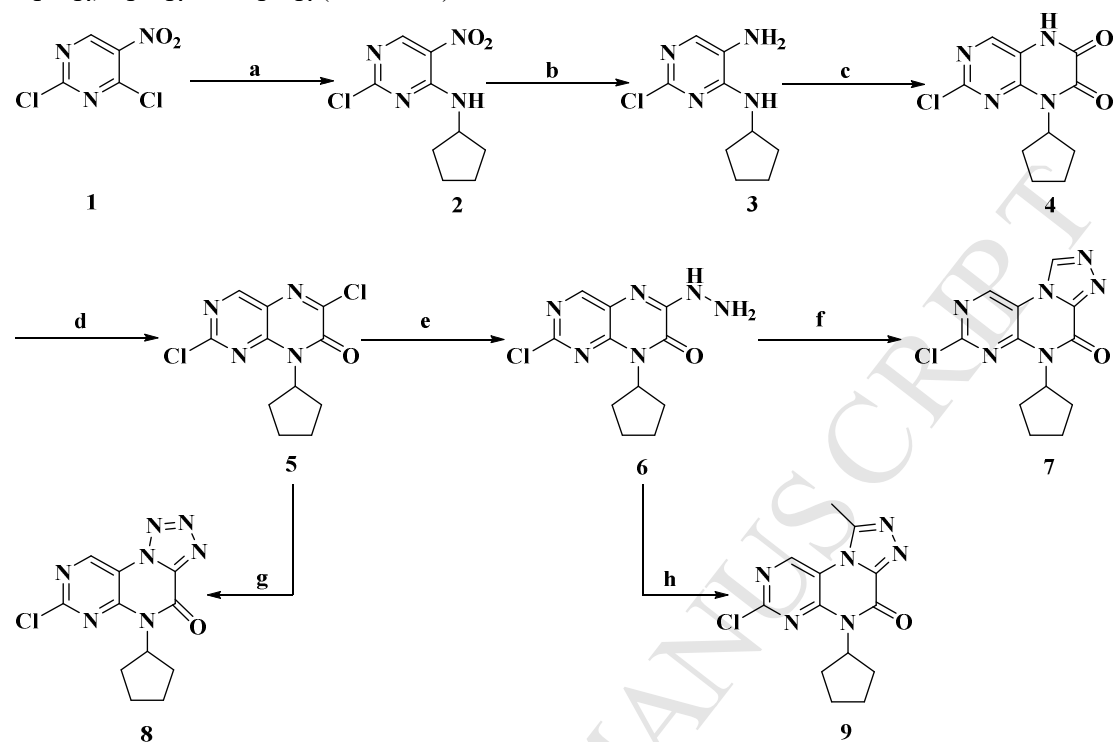
In this study, two series of novel 7-amino-[1,2,4]triazolo[4,3-*f*]pteridinone, and 7-aminotetrazolo[1,5-*f*]pteridinone derivatives were firstly designed and synthesized. All compounds were subsequently assayed for anti-proliferative activities *in vitro* against five cancer cell lines A549, PC-3, HCT116, MCF-7 and MDA-MB-231. Based on the anti-proliferative results, potent compounds were selected for further *in vitro* enzymatic inhibitory studies. To further clarify the primary mechanism, **L**₇ was taken forward and examined by *in vitro* AO/EB dyeing, the migration of A549 cells and cell cycle analysis.

2. Results and discussion

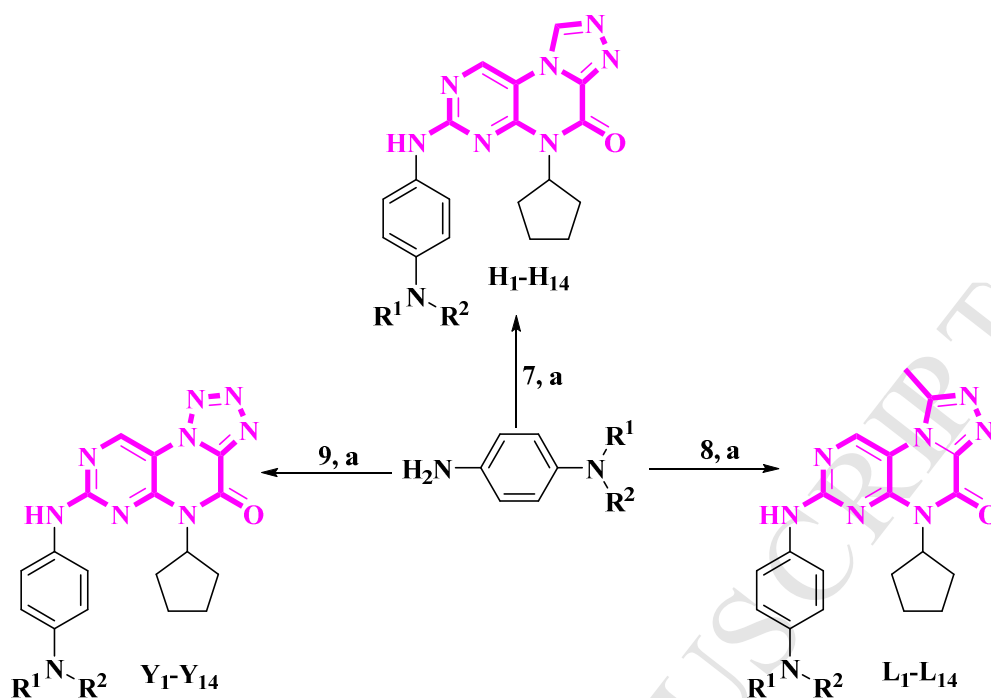
2.1 Chemistry

The general synthetic routes of the title compounds are illustrated in **Scheme 1-3**. Commercially available 2,4-dichloro-5-nitropyrimidine (**1**) as the starting material reacted with cyclopentylamine to give compound **2**, which was reduced using iron powder and catalytic amounts of concentrated HCl in EtOH/H₂O to obtain amide intermediate **3**. The intermediate **4** was prepared from **3** by treatment with ethyl oxalyl monochloride in acetone. Intermediate **4** was converted to chloro-pteridinone **5** by refluxing in SOCl₂ and catalytic amounts of DMF. Intermediate **5** was converted to tetrazole product **8** using NaN₃ as a cyclization reagent in DMF at 0 °C. Subsequently, the intermediate **6** was available *via* hydrazinolysis of intermediate **5** with 80% hydrazine monohydrate in EtOH at 40 °C. Intermediate **6** was treated with trimethyl orthoformate or triethyl orthoformate under 80 °C to produce triazole intermediates **7** and **9**, respectively. Side chain anilines (**12**) were prepared in two steps as shown in **Scheme 2**. Aromatic nucleophilic substitution of fluorine in 4-fluoronitrobenzene by secondary amines were readily achieved in DMF at 40 °C. The resulting nitrobenzenes were reduced to anilines using Pd/C in EtOH and

generally used without further purification. Subsequently, amination of **7**, **8**, and **9** by corresponding aryl amines (**12**) with *p*-toluenesulfonic acid as catalyst furnished target compounds **H₁-H₁₄**, **Y₁-Y₁₄** and **L₁-L₁₄** (**Scheme 3**).



Scheme 2. Preparation of the side chain anilines; Reagents and conditions: (a) Amines R¹R²NH, K₂CO₃, DMF, 40 °C, 6 h; (b) H₂, 10 % Pd/C, EtOH, rt, 5 h.



Scheme 3. General scheme for the synthesis of target compounds; Reagents and conditions: (a) *p*-Toluenesulfonic acid, 1-butanol, 100 °C, 15 h.

Alternatively, the key Intermediate **5** existed two reaction sites in the pteridinone structure (2-chlorine or 6-chlorine), which both could react with NaN_3 . So the tetrazole products **8** or **8a**, and the substitute products **8b** or **8c** could be obtained in theory (Fig. 5). In this sense, literature precedent illustrating the possibility of using this behavior for the generation of tetrazole products in which the methods of structure verification are rare. [26] Our efforts represent the first studies on the structure verification by X-ray single crystal. To our delight, the single product was finally achieved, and the X-ray single crystal diffraction analysis of this product (Fig. 6) permitted the assignment of its absolute configuration as 6-cyclization product **8** (CCDC: 1848418). Meanwhile, in the process of triazole product, the products **7** or **7a** could be obtained in theory. But the same result was achieved and the structure was confirmed by the X-ray single crystal diffraction as 6-cyclization product **7** (CCDC: 1848417). These results indicated that cyclization in 6-position of pteridinone was more reactive than the 2-position.

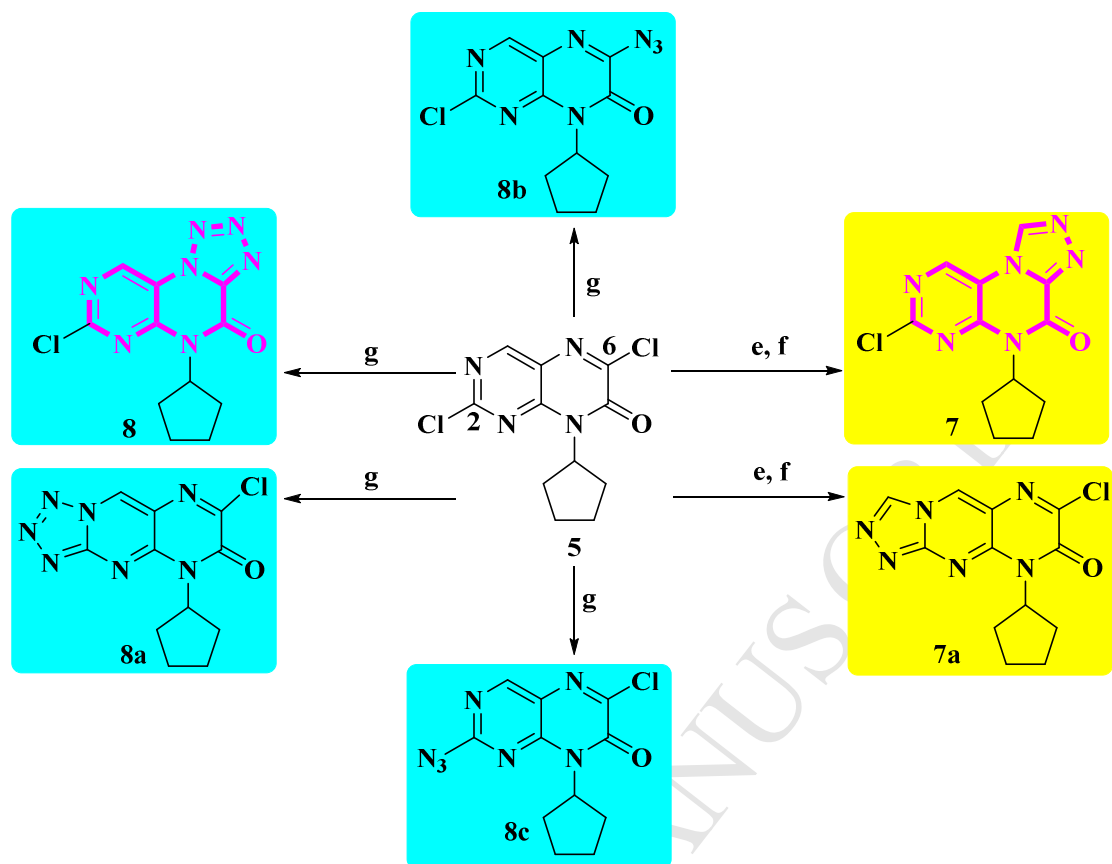


Fig. 5. The analysis of the cyclization products (tetrazole products **8**, **8a**, **8b**, **8c** and triazole products **7**, **7a**) of intermediate **5** in theory.

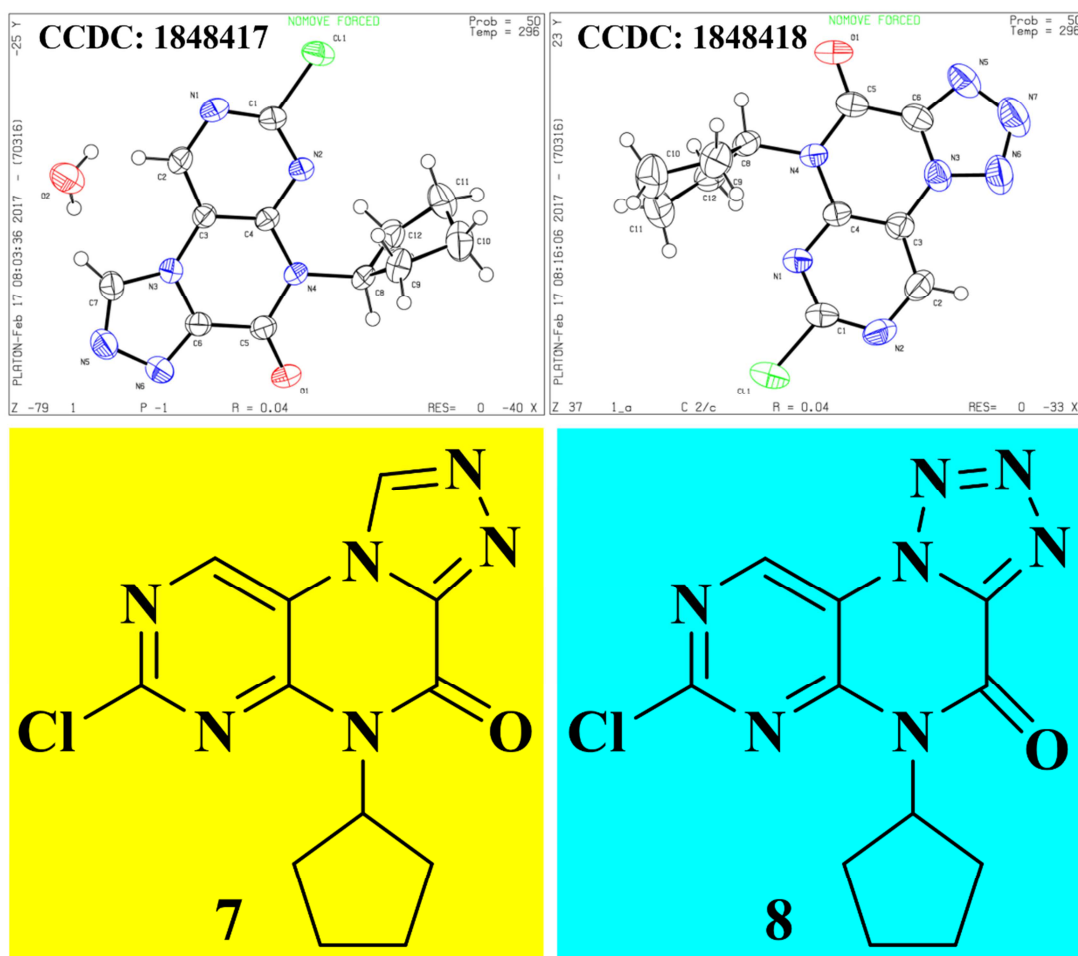
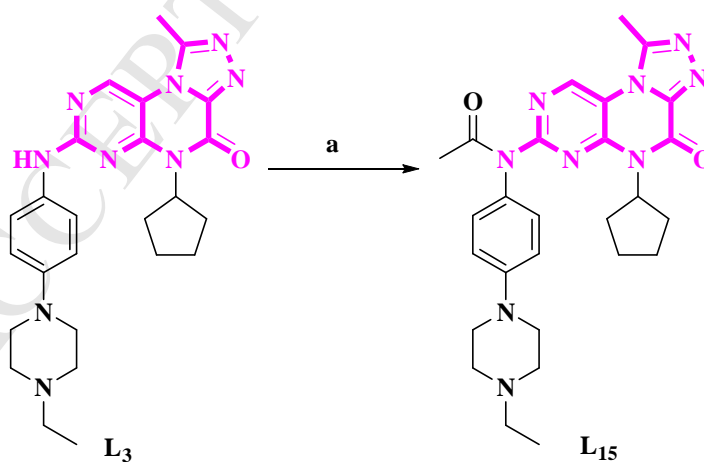


Fig. 6. X-ray crystal structure of compounds **7** and **8**.

Later, we evaluated the role of NH proton at the C-7 position of **L₃** in cytotoxicity assays by acylating **L₃** with acetic anhydride to obtain **L₁₅** (**Scheme 4**).



Scheme 4. Acylation of NH group of **L₃**; Reagents and conditions: (a) (Ac)₂O, 100 °C, 4h.

2.2 Bioactivity and discussion

2.2.1 *In vitro* antiproliferative activity and SARs study

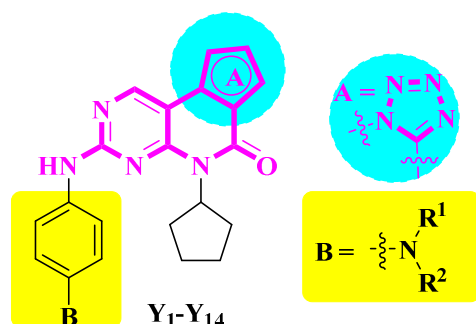
To evaluate *in vitro* antitumor activities, all synthesized compounds (**H₁-H₁₄**, **Y₁-Y₁₄**, and **L₁-L₁₅**) were investigated against a panel of cancer cell lines, including A549 (human lung adenocarcinoma), HCT116 (human colorectal cancer), PC-3 (human prostate cancer), MCF-7

(human breast cancer), MDA-MB-231 (human breast cancer) cells by the MTT assay. Meanwhile, palbociclib and BI6727 were served as positive controls. The results were expressed as half-maximal inhibitory concentration (IC_{50}) values and summarized in **Table 1**, **Table 2**, and **Table 3**. As illustrated in **Table 1**, most of 7-amino-[1,2,4]triazolo[4,3-*f*]pteridinone derivatives **H₁-H₁₄** showed moderate to significant cytotoxic activities against the different cancer cell lines. Several of these compounds were more potent than palbociclib against one or more cancer cell lines, which suggested that the combination of 2-aminopteridinone framework and triazolo moiety exhibit potent synergistic antitumor effect. Preliminary SARs indicated that the introduction of different amino groups at the C-7 position of 7-amino-[1,2,4]triazolo[4,3-*f*]pteridinone moiety had a significant influence on activity, which suggested that the hydrophilic **B** group contributed much to their potency. Compounds bearing piperazine moiety (**H₂**, **H₃**, **H₇**, and **H₉**) displayed excellent anti-tumor activities in the single-digit micromolar range against A549 and HCT116 cells. Notably, the better promising compound **H₇** displayed stronger potency than palbociclib in A549, HCT116 and MCF-7 cells with IC_{50} values of 0.89 μ M, 4.40 μ M and 0.41 μ M, respectively. However, when the piperazine was substituted by cyclopentyl (**H₁₃**), the cytotoxic activities decreased significantly. Replacement of the nitrogen atom of piperazine group in **H₇** by oxygen, carbon or sulfur atom (**H₁**, **H₄** and **H₈**) led to the diminished potency, indicating that the presence of cationic nitrogen atom was a critical factor in anti-proliferative activities. In order to improve the polarity of piperidine ring, hydrophilic hydroxyl group or *N*-methylpiperazinyl was embeded on the piperidine ring. The results indicated that the hydrophilic *N*-methylpiperazinyl (**H₁₄**) had more positive impact on the activities than hydroxyl group (**H₁₀**). Generally, five-membered pyrrolidine analogs were less active than corresponding six-membered inhibitors (**H₆** vs. **H₄**) despite possessing equivalently basic nitrogen atoms, highlighting the importance of ring size. Besides, an increase in potency was observed once the pyrrolidine group in **H₆** was "opened" to dimethylamine (**H₁₂**). Overall, SARs studies identified the 7-amino-[1,2,4]triazolo[4,3-*f*]pteridinone moiety bearing piperazine "tails" moieties harboring cationic nitrogen atoms with favorable potency.

Further studies were performed to examine the effect of shifting the 1,2,3-triazole motif of **H₁-H₁₄** series compounds to the tetrazolo series compounds (**Y₁-Y₁₄**). The results displayed that most of the tetrazolo series compounds had lower cytotoxicity than 1,2,3-triazole series. Interestingly, **Y₇** was maintained approximately cytotoxicity in A549, HCT116, PC-3, MCF-7 and MDA-MB-231 cells with IC_{50} values of 0.44 μ M, 0.60 μ M, 1.00 μ M, 0.50 μ M, and 1.60 μ M, respectively.

The methyl group acts as an essential factor in the molecular recognition of endogenous and exogenous substrates by means of bioreceptors. Although it only participates in London dispersion interactions, methyl group has stereoelectronic effects on micromolecules and biomacromolecules. Accordingly, the methyl group can lead to multiple biological effects, such as, selectivity among bioreceptors, increased the binding affinity, and protection against enzyme metabolism.[27] Further investigations were performed to study the introduction of a methyl group to the 1 position of 7-amino-[1,2,4]triazolo[4,3-*f*]pteridinone core on the cytotoxic activity. Piperazine "tails" moieties on the 7 position of 7-amino-1-methyl-[1,2,4]triazolo[4,3-*f*]pteridinone core to a proper degree was a key factor in improving inhibitory activity (**L₇** vs. **H₇**, **L₃** vs. **H₃**) suggesting that the methyl group was a favorable motif to potency in these cell lines.

Obviously, all target compounds possessed selectivity for A549 and HCT116 cancer cell lines,



Compd.	-NR ¹ R ²	IC ₅₀ ^a (μM) ± SD ^b				
		A549	HCT116	PC-3	MCF-7	MDA-MB-231
Y₁		4.81±0.02	43.23±0.02	>50	>50	48.45±0.09
Y₂		1.25±0.04	19.11±0.04	3.80±0.09	>50	15.81±0.08
Y₃		3.57±0.03	>50	16.12±0.06	>50	>50
Y₄		1.16±0.02	>50	>50	>50	>50
Y₅		4.92±0.08	>50	>50	>50	>50
Y₆		7.86±0.03	>50	>50	>50	>50
Y₇		0.44±0.01	0.60±0.01	1.00±0.03	0.50±0.03	1.60±0.04
Y₈		>50	>50	>50	>50	37.35±0.08
Y₉		3.85±0.04	>50	>50	2.31±0.02	>50
Y₁₀		>50	36.34±0.09	>50	>50	53.45±0.09
Y₁₁		>50	43.22±0.08	>50	>50	8.95±0.03
Y₁₂		10.06±0.09	>50	>50	2.58±0.05	>50
Y₁₃		>50	2.12±0.04	>50	>50	>50
Y₁₄		1.28±0.01	7.62±0.03	>50	>50	5.81±0.03
Palbociclib		1.32±0.02	8.90±0.05	2.20±0.02	4.09±0.05	3.50±0.03
BI6727		0.08±0.01	0.11±0.02	0.09±0.01	0.09±0.02	0.11±0.03

^a Values are the means of at least three independent experiments. ^b SD: standard deviation.

Table 3. Structures and cytotoxicity of compounds (**L₁-L₁₄**).

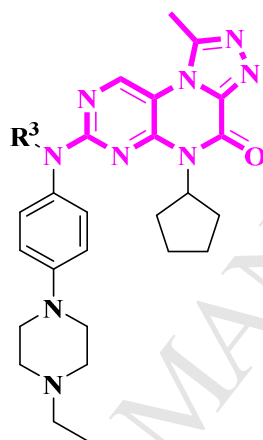


Compd.	-NR ¹ R ²	IC ₅₀ ^a (μM) ± SD ^b				
		A549	HCT116	PC-3	MCF-7	MDA-MB-231
L₁		4.29±0.02	8.91±0.02	>50	>50	>50
L₂		1.92±0.05	72.82±0.05	7.61±0.08	1.05±0.02	0.61±0.03
L₃		0.68±0.03	9.61±0.03	5.00±0.05	0.51±0.02	2.25±0.01
L₄		5.24±0.07	19.11±0.07	>50	>50	6.26±0.05
L₅		>50	11.23±0.08	>50	>50	>50
L₆		>50	>50	>50	>50	>50

L₇		0.16±0.02	0.30±0.03	0.51±0.02	0.30±0.01	0.70±0.02
L₈		7.19±0.08	5.82±0.01	>50	>50	>50
L₉		5.46±0.03	7.61±0.05	8.44±0.01	0.75±0.01	3.35±0.04
L₁₀		21.69±0.09	18.12±0.03	>50	>50	>50
L₁₁		9.29±0.06	>50	>50	>50	>50
L₁₂		8.86±0.04	29.11±0.02	>50	>50	>50
L₁₃		11.36±0.04	>50	>50	>50	9.12±0.07
L₁₄		2.38±0.05	12.12±0.03	>50	3.21±0.03	5.85±0.09
Palbociclib		1.32±0.02	8.90±0.05	2.20±0.02	4.09±0.05	3.50±0.03
BI6727		0.08±0.01	0.11±0.02	0.09±0.01	0.09±0.02	0.11±0.03

^a Values are the means of at least three independent experiments. ^b SD: standard deviation.

Table 4. *In vitro* cytotoxicity of **L₃** and **L₁₅** Compounds



Compd.	R ³	IC ₅₀ ^a (μM) ± SD ^b				
		A549	HCT116	PC-3	MCF-7	MDA-MB-231
L₃	H	0.68±0.03	9.61±0.03	5.00±0.05	0.51±0.02	2.25±0.01
L₁₅	CH ₃ CO-	20.25±0.09	40.32±0.08	>50	>50	>50

^a Values are the means of at least three independent experiments. ^b SD: standard deviation.

According to the literatures [14], the NH of the 7 position at 7-aminopteridinone core acted as a key hydrogen bond donor to interact with the corresponding amino acids in the kinase hinge region. As hypothesized, amine-substituted anilines (**L₁₅**) positioned at C7 of the 7-amino-1-methyl-[1,2,4]triazolo[4,3-f]pteridinone core led to an inactive compound. This was not surprising for this bridging NH may act as a key hydrogen bond donor.

2.2.2 *In vitro* enzymatic assays

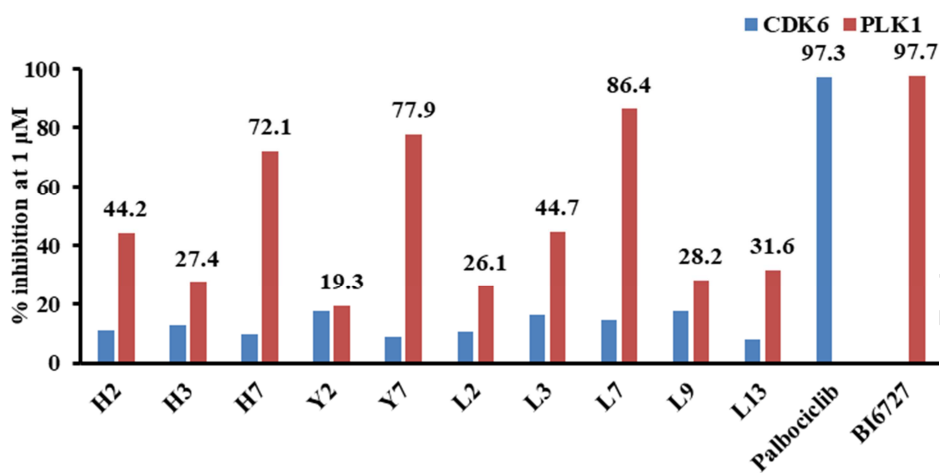


Fig. 7. Enzymatic activities of the target compounds.

Based on the cellular assays and molecular docking results, potent compounds were selected for further *in vitro* CDK6, and PLK1 % inhibition at 1 μ M. The results were summarized in **Fig. 7**. As shown in **Fig. 7**, all compounds poorly inhibited CDK6 kinases with % inhibition values ranging from 8.9% to 17.6%. However, most of compounds displayed more highly inhibition against PLK1 than CDK6 kinases with % inhibition values ranging from 19.3% to 86.4%. In parallel with cellular results, inhibitors bearing the 1-methyl-1,2,4-triazole at **A** ring of pteridinone core were found to more potent than corresponding 1,2,4-triazole or tetrazolo analogues, which further proved 7-amino-1-methyl-triazolo[4,3-*f*]pteridin-4(5*H*)-one a favorable building block to increase PLK1 potency. Even though it showed more selectivity against PLK1, the inhibitory activity of compound **L**₇ was still less than BI6727. These results indicated that two series of novel compounds worth further studying as new potential anticancer agent for the treatment of human cancers.

2.2.3 Cell apoptosis study

To investigate the molecular mechanisms of action preliminarily, cell apoptosis analysis of A549 cells treated with the optimal compounds **Y**₇ and **L**₇ was performed using a biparametric acridine orange (AO) and ethidium bromide (EB) staining. EB was able to penetrate through intact membranes of live cells and colors DNA as green fluorescence, while AO was only taken up by apoptotic cells with damaged membranes coloring DNA as orange fluorescence. Therefore, normal live cells appeared uniformly stained green in color. Early apoptotic cells contained bright green condensed bodies in their nuclei representing nuclear DNA fragmentation and later apoptotic cells presented colored orange nuclei indicating that their membranes are broken.

As shown in **Fig. 8**, orange-red stained cell nucleus appeared after treatment with 1.0 μ M compound **Y**₇ and **L**₇ for 24 h, indicating the late stage apoptosis of A549 cells. Treatment with 5.0 μ M compound **Y**₇ and **L**₇ led to a significant increase in the percentage of apoptotic cells, marked by concentrated orange-red nucleus stained with EB. In addition, these results demonstrated that compound **L**₇ was more potent than **Y**₇ in inducing cell apoptosis, indicating that compound **L**₇ deserves further investigation.

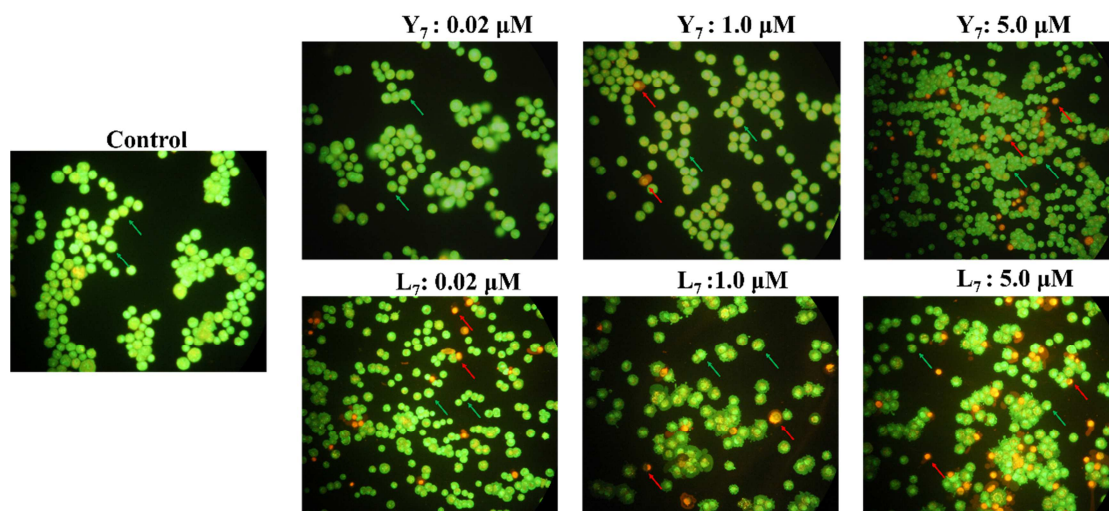


Fig. 8. Effect of compound Y₇ and L₇ on cell apoptosis in A549 cells.

2.2.4 Wound-healing assay.

As migration is an important characteristic for metastatic cancers, the effect of compound L₇ on migration of cancer cells was investigated by the wound healing assay. As shown in **Fig. 9** and **10**, treatment of A549 cells with compound L₇ at indicated concentrations markedly suppressed the wound healing in a concentration-dependent manner.

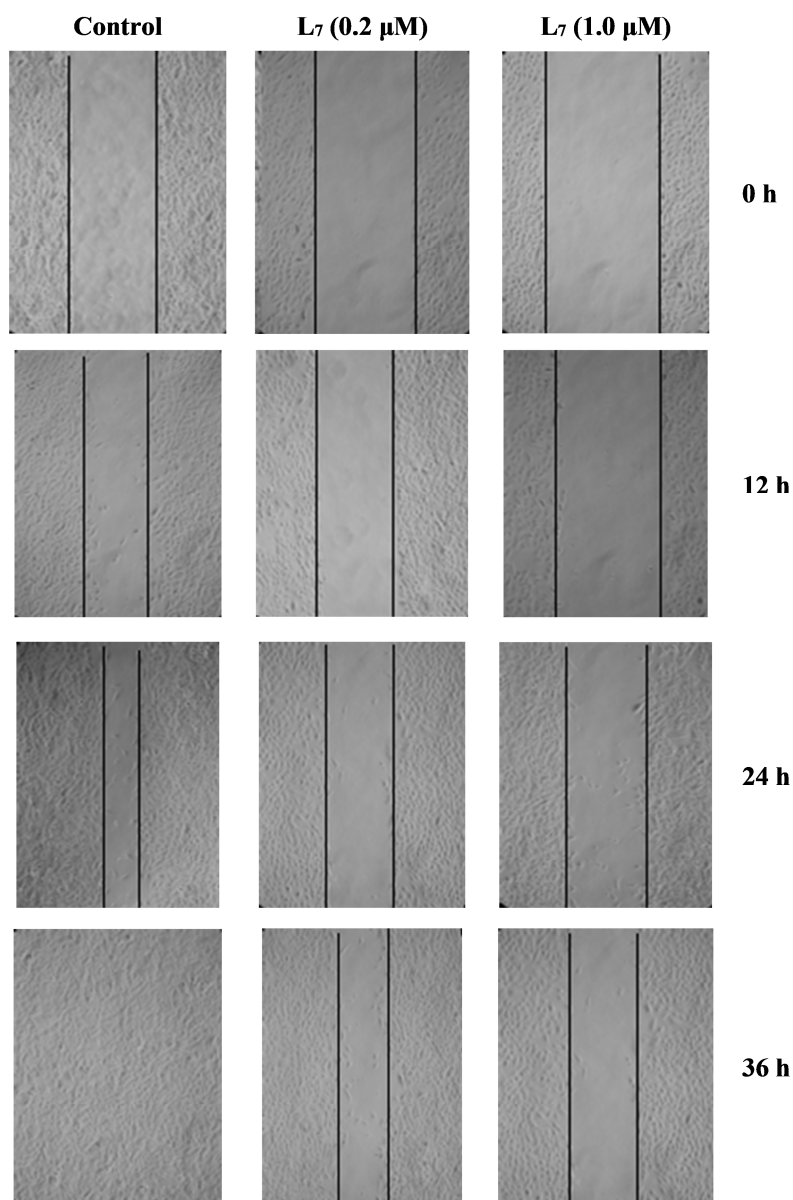


Fig. 9. *In vitro* wound healing assay on A549 cells. Phase contrast images were obtained by the treatment of compounds L₇ at indicated concentrations for 0, 12, 24 and 36 h.

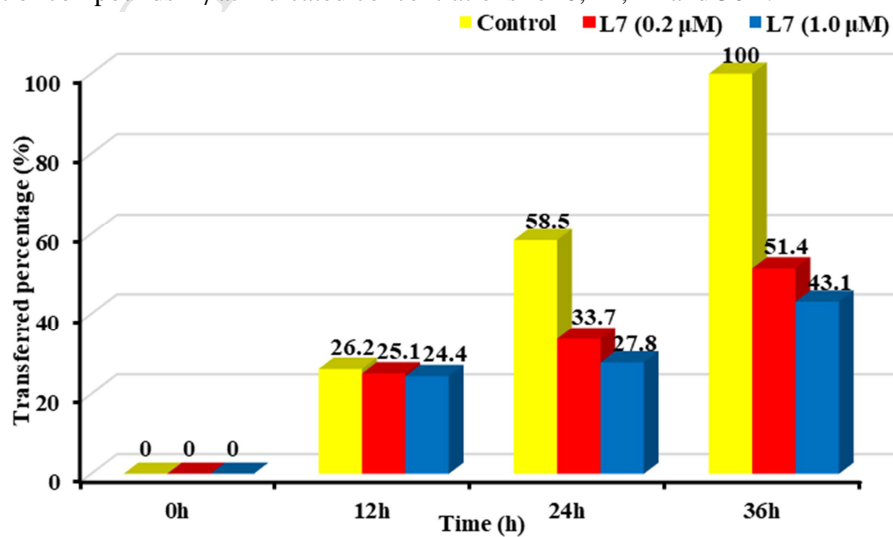


Fig. 10. *In vitro* wound healing on A549 cells of **L₇**. Columnar graph represents the transferred percentage distribution at different concentrations and at different time.

2.2.5 Cell cycle analysis

The cell cycle analysis was performed to investigate the prevention of proliferation in A549 cells with the most potent compound **L₇**. After treatment of A549 cells with compound **L₇** for 24 h at indicated concentrations (0.2, 1.0, 5.0 μM), the cells were fixed and stained with PI, the DNA content was analyzed by flow cytometry. The obtained results were compared with non-treated A549 cells, as control. As shown in **Figs. 11** and **12**, treatment of A549 cells with **L₇** at 0.2, 1.0, and 5.0 μM concentrations increased the percentage of G1-phase cells from 63.34% (as control group) to 74.99%, 79.82%, and 82.32%, respectively. These results confirmed that compound **L₇** significantly caused G1-phase arrest in A549 cells.

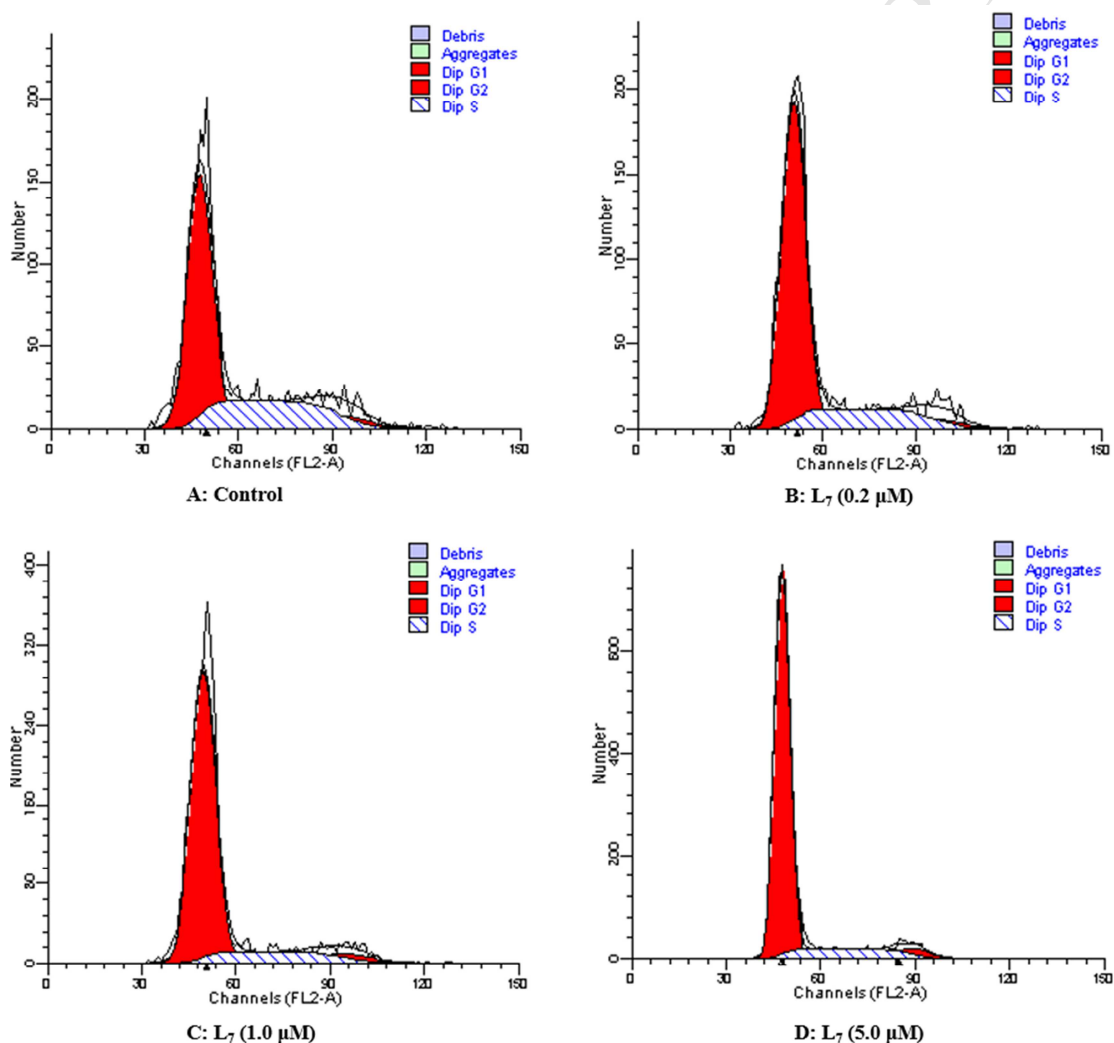


Fig. 11. Effect of compound **L₇** on the cell cycle distribution of A549 cells.

Fig. 13. The binding models of **L₇** or **L₁₅** with PLK1 and CDK6. (A) Predicted binding conformation for **L₇** (blue sticks) in the binding site cavity of PLK1 (PDB code: 3FC2), (B) 2D diagram of the interaction between **L₇** and the binding site cavity of PLK1, (C) **L₇** overlapping with BI6727 (red sticks), (D) 2D diagram of the interaction between **L₇** (pink sticks) and the binding site cavity of CDK6 (PDB code: 5L2I), (E) **L₇** overlapping with palbociclib, (F) 2D diagram of the interaction between palbociclib (green sticks) and the binding site cavity of CDK6, (G) 2D diagram of the interaction between **L₁₅** (dark green sticks) and the binding site cavity of PLK1, and (H) 2D diagram of the interaction between **L₁₅** and the binding site cavity of CDK6.

In order to better understand the binding mode, molecular docking models of **L₇** or **L₁₅** were performed based upon the cocrystal structure of PLK1 with BI6727 (PDB code: 3FC2) and CDK6 with palbociclib (PDB code: 5L2I), respectively.

As shown in **Fig. 13**, **L₇** occupied the kinase domain in a similar manner to BI6727. In contrast to two hydrogen bonds observed in the cocrystal structure of BI6727 with PLK1 (**Fig. 13A**) at the hinge area, **L₇** was found to form three hydrogen bonds *via* the 8-position nitrogen atom, the 7-position NH and the 4-position oxygen atom of carbonyl of the 7-amino-1-methyl-[1,2,4]triazolo[4,3-*f*]pteridinone nuclei with Cys 133 and Cys 67, respectively (**Fig. 13A**). In the meantime, the π -Sigma interaction between triazolo with Leu 130 and the π - π stacked interaction between [1,2,4]triazolo[4,3-*f*]pteridinone with Phe 183 was also present. Inspiringly, the hydrophilic "tail", 2,6-dimethylpiperazine moiety, was engaged in π -alkyl interactions and carbon hydrogen bonds with Leu 59, validating the rationality of our design and the importance of the basic nitrogen atoms (**Fig. 13B**). Besides, its 1-position methyl group on the triazolo moiety filled with active chamber which would be beneficial to increase the binding affinity. All these interactions played an important role in stabilizing the conformation of ligand-protein complex. Docking structure of compound **L₇** overlaid with BI6727 in PLK1 showed that the conformation and binding mode of compound **L₇** were well consistent with BI6727 (**Fig. 13C**). Although **L₇** occupied the kinase domain in a similar manner to palbociclib (**Fig. 13E**), palbociclib was found to form three hydrogen bonds *via* the 3-position nitrogen atom, the 2-position NH and the 6-position oxygen atom of acetyl of the pyridin-2-yl)amino)pyrido[2,3-*d*]pyrimidin-7(8H)-one nuclei with Val 101 and Asp 163, respectively (**Fig. 13F**), compared to **L₇** was found to form only two hydrogen bonds with Val 101 (**Fig. 13D**).

On the other hand, the docking results of compound **L₁₅** suggested that the acetylated 7 position N atom could not form hydrogen bond with Cys 133 of PLK1 protein, and with Val 101 of CDK6 protein. Meanwhile, the introduction of acetyl group resulted the forming of unfavorable bump. Therefore, the NH of the 7 position at 7-aminopteridinone core played an important role. This result was also consisted with the *in vitro* antiproliferative activity, which the acetylated product **L₁₅** displayed lower potency than compound **L₃**. Therefore, the 7-amino-1-methyl-[1,2,4]triazolo[4,3-*f*]pteridinone moiety could serve as a scaffold from which to build a novel series of PLK1 inhibitors.

2.3 Physicochemical and ADME parameters

Furthermore, some physicochemical and ADME properties of the synthesized compounds and positive controls were predicted using the SwissADME (a free web tool to evaluate pharmacokinetics, drug likeness and medicinal chemistry friendliness of small molecules) for their adaptability with Lipinski's rule of five [28-32]. Compounds obeying at least three of the four criteria are considered to adhere to Lipinski Rule.

As demonstrated in **Table 5**, the most active compounds shown variable permeability based on

gastrointestinal absorption (GI), according to the BOILED-Egg predictive model (Brain Or IntestinaL EstimatedD permeation method). All predicted compounds showed high gastrointestinal absorption. With respect to oral bioavailability, it's expected 0.55 of probability of oral bioavailability score >10% in the rat for all compounds, greater than BI6727 (0.17). Compound **L₇** exhibited potent *in vitro* antitumor activity, low toxicity and reasonable physicochemical properties, because suitable flexible and size in the bioavailability radar map (**Fig. 14**). All these data suggests that compound **L₇** could be considered as a promising candidate for further development.

Table 5. Physicochemical properties and ADME properties of most active compounds.

Compd.	MW (g/mol)	H-bond acceptors	H-bond donors	Log P o/w	Violation Lipinski Rule of 5	^a PSA (Å ²)	Rotatable bonds	^b BBB	^c GI	^d BS
H₇	459.55	6	2	2.06	0	105.27	4	NO	High	0.55
Y₇	460.53	7	2	2.11	1	118.16	4	NO	High	0.55
L₇	473.57	6	2	2.40	0	105.27	4	NO	High	0.55
H₃	459.55	6	1	2.10	0	96.48	5	NO	High	0.55
Y₃	460.53	7	1	2.16	1	109.37	5	NO	High	0.55
L₃	473.57	6	1	2.46	0	96.48	5	NO	High	0.55
L₉	489.57	7	2	1.78	1	116.71	6	NO	High	0.55
L₁₄	542.68	7	1	2.47	2	99.72	5	NO	High	0.17
Palbociclib	447.53	6	2	2.24	0	105.04	5	NO	High	0.55
BI6727	618.81	7	2	3.59	2	106.17	11	NO	High	0.17

^aPSA - Polar surface area. ^bBBB - blood-brain barrier. ^cGI - Gastrointestinal absorption. ^dBS - Bioavailability Score.

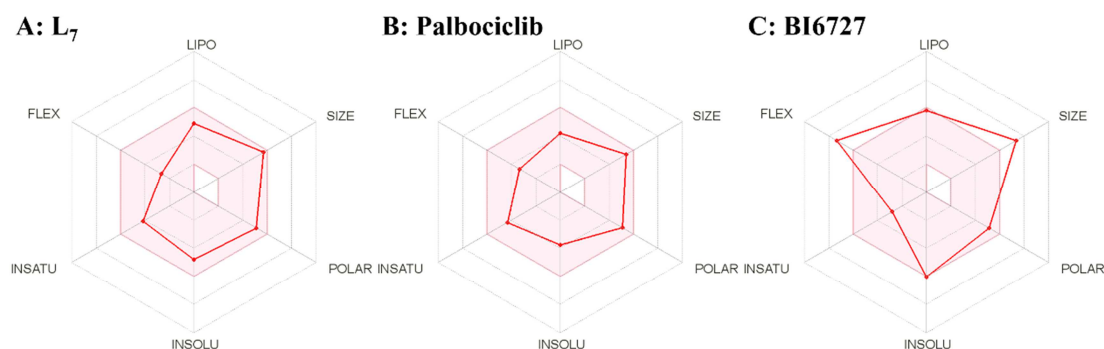


Fig. 14. The bioavailability radar enables a first glance at the drug-likeness of a molecule (**A: L₇**, **B: Palbociclib**, **C: BI6727**). The pink area represents the optimal range for each properties (lipophilicity: XLOGP3 between -0.7 and +5.0, size: MW between 150 and 500 g/mol, polarity: TPSA between 20 and 130 Å², solubility: log *S* not higher than 6, saturation: fraction of carbons in the sp³ hybridization not less than 0.25, and flexibility: no more than 9 rotatable bonds).

3. Conclusion

In current investigation, two series of novel 7-amino-[1,2,4]triazolo[4,3-*f*]pteridinone, and 7-aminotetrazolo[1,5-*f*]pteridinone derivatives with hydrophilic "tails" (**B**) bearing aliphatic amine groups, were firstly designed and synthesized. Exploration of SARs culminated in **L₇**, which contained a terminal 2,6-dimethylpiperazine at **B** and 1-methyl-1,2,4-triazole at **A** ring of pteridinone core, showed the most potent antiproliferative activity against A549, PC-3, HCT116, MCF-7 and MDA-MB-231 cell lines with IC₅₀ values of 0.16 μM, 0.30 μM, 0.51 μM, 0.30 μM, and

0.70 μM , respectively. Combined with the results of the molecular docking and enzymatic studies, the PLK1 was very likely to be one of the drug targets of compound **L7**. Furthermore, to clarify the mechanism of the anticancer activity of the pteridinone molecule, the AO/EB and wound-healing assays confirmed that **L7** induced cell apoptosis. Finally, cell cycle analysis of **L7** by flow cytometry showed cell cycle arrest in G1 phase, DNA fragmentation and alteration in mitochondrial membrane potential by compound **L7** for the three concentrations tested. In summary, the SARs studies together with the pharmacological assays on novel pteridin-4(5H)-one analogues identified **L7** as a promising anti-cancer agent, which will lead to the promising development of new drugs.

4. Experimental procedures

4.1 Chemistry

All melting points were acquired on a Mettler Melting Point MP70 apparatus (Mettler, Toledo, Switzerland) and uncorrected. Mass spectra (MS) were taken in ESI mode on Agilent 1100 LC-MS (Agilent, Palo Alto, CA, USA). Reactions were monitored by thin-layer chromatography (TLC) on silica plates (F-254) and visualized under UV light. ^1H NMR and ^{13}C NMR spectra were performed using Bruker spectrometers (Bruker Bioscience, respectively, Billerica, MA, USA) with TMS as an internal standard. Column chromatography was run on silica gel (200-300 mesh) from Qingdao Ocean Chemicals (Qingdao, Shandong, China). X-Ray diffraction studies were carried on an Bruker SMART Apex-II CCD-based X-ray diffractometer. Unless otherwise noted, all materials were obtained from commercially available sources and used without further purification.

4.1.1 General procedure for preparation of compounds (2-9)

4.1.1.1 2-chloro-N-cyclopentyl-5-nitropyrimidin-4-amine (2)

2,4-Dichloro-5-nitropyrimidine (50.0 g, 259 mmol) and NaHCO_3 (43.5 g, 518 mmol) were dissolved in DCM (200 mL) and cooled to 0 $^\circ\text{C}$. Cyclopentylamine (26.4 g, 311 mmol) was dissolved in DCM (50 mL) and added dropwise. After the completion of the dropwise addition, the cooling bath was removed, and the reaction mixture was stirred at room temperature for about 10 h. Then organic was washed by water, and brine. The organic phase was dried over Na_2SO_4 , filtered, and the solvent evaporated to obtain 53.27 g of **2** as a yellow solid, m.p.: 125.2 – 126.6 $^\circ\text{C}$. Yield: 85%; MS (ESI) m/z : 243.3 $[\text{M}+\text{H}]^+$.

4.1.1.2 2-chloro-N4-cyclopentylpyrimidine-4,5-diamine (3)

To a suspension of compound **2** (50.0 g, 207 mmol) in 200 mL of 95% ethanol was added HCl (1 mL), and Fe Powder (57.8 g, 1035 mmol) in batches. The mixture was heated for 2 h at reflux. After completion of the reaction as indicated by TLC, the mixture was filtered through a celite bed and concentrated in a vacuum to afford pure product. The residue was purified by silica gel column chromatography to obtain 32.1 g of **3** as a white solid, m.p.: 128.2 – 130.0 $^\circ\text{C}$. Yield: 73.3%; MS (ESI) m/z : 213.2 $[\text{M}+\text{H}]^+$.

4.1.1.3 2-chloro-8-cyclopentyl-5,8-dihydropteridine-6,7-dione (4)

To a stirred solution of compound **3** (30.0 g, 124 mmol) and K_2CO_3 (34.2 g, 248 mmol) in acetone (150 mL) was dropped ethyl oxalyl monochloride (28.9 g, 136 mmol). The mixture was stirred at rt for 2 h. The reaction mixture was filtered and the filtrate was concentrated under reduced pressure. The crude ketoester was dissolved in absolute EtOH (200 mL), placed in a pressure flask, and TEA (15.1 g, 149 mmol) was added. The mixture was heated for 4 h at 100 $^\circ\text{C}$. After completion of the reaction as indicated by TLC, the mixture was filtered to obtain 27.4 g of **4** as a

white solid, m.p.: 210.1 – 212.2 °C. Yield: 83.6%; MS (ESI) m/z : 264.9 [M-H]⁻.

4.1.1.4 2,6-dichloro-8-cyclopentylpteridin-7(8H)-one (**5**)

To a solution of compound **4** (25.0 g, 94 mmol) in SOCl₂ (80 mL) at reflux was dropped DMF (1 mL), and the resulting mixture was kept at this temperature for 2 h. The solvent was concentrated in vacuum and the residue was poured into stirring ice-water (200 mL), the resulting precipitate was filtered and dried to obtain 24.3 g of **5** as a white solid, m.p.: 269.0 – 279.3 °C. Yield: 91.2%; MS (ESI) m/z : 285.26 [M+H]⁺.

4.1.1.5 2-chloro-8-cyclopentyl-6-hydrazinylpteridin-7(8H)-one (**6**)

A mixture of **5** (18.0 g, 63.4 mmol) and 80% hydrazine monohydrate (9.5 g, 190 mmol) in EtOH (200 mL) was stirred at 40 °C for 2h. After completion of the reaction as indicated by TLC, most of the solvent was evaporated under reduced pressure when white solid appeared. The resulting precipitate was filtered off, washed with water, and dried under vacuum to afford 15.6 g of **6** as a white solid, m.p.: 210.7 – 212.1 °C. Yield: 88.4%; MS (ESI) m/z : 279.0 [M-H]⁻.

4.1.1.6 7-chloro-5-cyclopentyl-[1,2,4]triazolo[4,3-f]pteridin-4(5H)-one (**7**)

To a stirred solution of compound **6** (6.0 g, 21.4 mmol) in trimethyl orthoformate (20 mL). The reaction mixture was stirred at 80 °C for 2h, cooled to room temperature. The resulting precipitate was filtered off, washed with diethyl ether, and dried to afford 5.3 g of **7** as a white solid, m.p.: 251.8 – 253.1 °C. Yield: 86.1%; MS (ESI) m/z : 313.1 [M+Na]⁺. ¹H NMR (400 MHz, DMSO-*d*₆) δ 9.90 (s, 1H), 9.49 (s, 1H), 5.76 – 5.60 (m, 1H), 2.21-2.13 (m, 2H), 2.09 – 1.98 (m, 2H), 1.98 – 1.83 (m, 2H), 1.67-1.64 (m, 2H).

4.1.1.7 7-chloro-5-cyclopentyltetrazolo[1,5-f]pteridin-4(5H)-one (**8**)

NaN₃ (1.14 g, 17.6 mmol) was added to suspension of **5** (5.0 g, 17.6 mmol) and DMF (20 mL). The mixture was stirred at 0 °C for 10 h. After completion of the reaction as indicated by TLC, the reaction mixture was cooled to room temperature. Water was then added, and the solid was filtered and dried under reduced pressure to afford 4.2 g of **8** as a white solid, m.p.: 185.4 – 186.8 °C. Yield: 80.2%; MS (ESI) m/z : 292.3 [M+H]⁺. ¹H NMR (400 MHz, DMSO-*d*₆) δ 9.71 (s, 1H), 5.78 – 5.70 (m, 1H), 2.21 – 2.13 (m, 2H), 2.08 – 2.02 (m, 2H), 2.00 – 1.88 (m, 2H), 1.73 – 1.62 (m, 2H).

4.1.1.8 7-chloro-5-cyclopentyl-1-methyl-[1,2,4]triazolo[4,3-f]pteridin-4(5H)-one (**9**)

To a stirred solution of compound **6** (6.0 g, 21.4 mmol) in triethyl orthoformate (20 mL). The reaction mixture was stirred at 80 °C for 2h, cooled to room temperature. The resulting precipitate was filtered off, washed with diethyl ether, and dried to afford 5.2 g of **9** as a white solid, m.p.: 255.3 – 257.1 °C. Yield: 79.1%; MS (ESI) m/z : 327.2 [M+Na]⁺.

4.1.2 General Procedure for Preparation of (**11**)

Substituted amine (1.2 equiv) was added to a mixture of 4-fluoronitrobenzene (1 equiv) and K₂CO₃ (2.0 equiv) in DMF (7 mL/g). The reaction mixture was stirred at 40 °C and followed by TLC. After completion of the reaction, the mixture was poured into stirring ice-water. The resulting precipitate was filtered and dried to obtain compounds **11** as a yellow solid.

4.1.3 General Procedure for Preparation of (**12**)

The substituted nitro compound **11** (1 equiv in a mixture of EtOH-H₂O, 95:5, 20 mL) was treated with 10% Pd-carbon (5% w/w). The reaction was subjected to hydrogenation under hydrogen gas at room temperature and the reaction was monitored by TLC. After completion of the reaction, the mixture was filtered through a Celite bed and concentrated in a vacuum to afford product **12**.

4.1.4 General procedure for preparation of compounds (**H**₁-**H**₁₄, **Y**₁-**Y**₁₄, **L**₁-**L**₁₄)

To a stirred solution of compound **7**, **8**, or **9** (1 equiv) in 1-butanol was added compounds **12** (1.1 equiv) and *p*-toluenesulfonic acid (1 equiv). The mixture was placed in a pressure flask, and heated to 100 °C for 15 h. The reaction mixture was quenched by saturated Na₂CO₃ aqueous solution, and then was extracted with DCM and the organic phase was washed with water, dried over anhydrous Na₂SO₄. The combined organic layer was concentrated under reduced pressure and was further purified by flash column chromatography using dichloromethane/methanol as eluent to afford product **H₁-H₁₄**, **Y₁-Y₁₄**, or **L₁-L₁₄** as a pale yellow solid.

5-cyclopentyl-7-((4-morpholinophenyl)amino)-[1,2,4]triazolo[4,3-f]pteridin-4(5H)-one (H₁)

Yield: 51.6%; m.p.: 315.3 – 316.5 °C; MS (ESI) *m/z*: 455.4 [M+Na]⁺; ¹H NMR (400 MHz, DMSO-*d*₆) δ 9.73 (s, 2H), 9.18 (s, 1H), 7.51 (d, *J* = 8.9 Hz, 2H), 6.94 (d, *J* = 9.0 Hz, 2H), 5.78 – 5.70 (m, 1H), 3.75 – 3.73 (m, 4H), 3.07 – 3.05 (m, 4H), 2.29 – 2.21 (m, 2H), 1.97 – 1.89 (m, 2H), 1.87 – 1.79 (m, 2H), 1.64 – 1.56 (m, 2H); Anal. Calcd for C₂₂H₂₄N₈O₂: C, 61.10; H, 5.59; N, 25.91; Found: C, 61.07; H, 5.51; N, 25.90.

5-cyclopentyl-7-((4-(4-methylpiperazin-1-yl)phenyl)amino)-[1,2,4]triazolo[4,3-f]pteridin-4(5H)-one (H₂)

Yield: 62.0%; m.p.: 304.5 – 305.7 °C; MS (ESI) *m/z*: 446.6 [M+H]⁺; ¹H NMR (600 MHz, DMSO-*d*₆) δ 9.75 – 9.73 (m, 2H), 9.19 (s, 1H), 7.49 (d, *J* = 6.3 Hz, 2H), 6.93 (d, *J* = 7.8 Hz, 2H), 5.74 (s, 1H), 3.09 (s, 4H), 2.45 (s, 4H), 2.25 (s, 2H), 2.22 (s, 3H), 1.93 (s, 2H), 1.83 (s, 2H), 1.60 (s, 2H); ¹³C NMR (101 MHz, DMSO-*d*₆) δ 158.14, 153.79, 153.38, 149.23, 147.49, 142.52, 139.88, 137.87, 131.88, 121.74, 116.18, 55.14, 53.76, 49.15, 46.27, 40.64, 40.43, 40.22, 40.02, 39.81, 39.60, 39.39, 28.15, 25.58; Anal. Calcd for C₂₃H₂₇N₉O: C, 62.01; H, 6.11; N, 28.30; Found: C, 61.98; H, 6.04; N, 28.28.

5-cyclopentyl-7-((4-(4-ethylpiperazin-1-yl)phenyl)amino)-[1,2,4]triazolo[4,3-f]pteridin-4(5H)-one (H₃)

Yield: 59.8%; m.p.: 318.7 – 320.0 °C; MS (ESI) *m/z*: 460.6 [M+H]⁺; ¹H NMR (600 MHz, DMSO-*d*₆) δ 9.73 (s, 2H), 9.17 (s, 1H), 7.48 (d, *J* = 8.2 Hz, 2H), 6.93 (d, *J* = 8.6 Hz, 2H), 5.74 (s, 1H), 3.32 (s, 3H), 3.09 (s, 4H), 2.37 – 2.35 (m, 2H), 2.29 – 2.20 (s, 2H), 1.93 (s, 2H), 1.84 – 1.79 (m, 2H), 1.64 – 1.56 (m, 2H), 1.03 (t, *J* = 7.1 Hz, 3H); ¹³C NMR (101 MHz, DMSO-*d*₆) δ 158.15, 153.38, 149.24, 147.55, 142.52, 137.84, 131.84, 121.79, 116.15, 108.64, 53.78, 52.86, 52.11, 49.28, 40.64, 40.43, 40.22, 40.01, 39.80, 39.59, 39.39, 28.14, 25.57, 12.48; Anal. Calcd for C₂₄H₂₉N₉O: C, 62.73; H, 6.36; N, 27.43; Found: C, 62.70; H, 6.31; N, 27.41.

5-cyclopentyl-7-((4-(piperidin-1-yl)phenyl)amino)-[1,2,4]triazolo[4,3-f]pteridin-4(5H)-one (H₄)

Yield: 48.3%; m.p.: 291.9 – 293.0 °C; MS (ESI) *m/z*: 429.6 [M-H]⁻; ¹H NMR (600 MHz, DMSO-*d*₆) δ 9.53 (s, 1H), 8.94 (s, 1H), 7.41 (d, *J* = 8.2 Hz, 2H), 6.53 (d, *J* = 8.8 Hz, 2H), 5.75 (s, 1H), 3.21 (t, *J* = 6.3 Hz, 4H), 2.91 (s, 2H), 2.25 – 2.20 (m, 2H), 1.95 – 1.91 (m, 4H), 1.89 – 1.88 (m, 2H), 1.85 – 1.78 (m, 2H), 1.61 – 1.55 (s, 2H); Anal. Calcd for C₂₃H₂₆N₈O: C, 64.17; H, 6.09; N, 26.03; Found: C, 64.13; H, 6.02; N, 26.01.

5-cyclopentyl-7-((4-(4-methylpiperidin-1-yl)phenyl)amino)-[1,2,4]triazolo[4,3-f]pteridin-4(5H)-one (H₅)

Yield: 55.6%; m.p.: 329.8 – 331.3 °C; MS (ESI) *m/z*: 445.5 [M+H]⁺; ¹H NMR (600 MHz, DMSO-*d*₆) δ 9.72 (s, 1H), 9.69 (s, 1H), 9.17 (s, 1H), 7.46 (d, *J* = 8.7 Hz, 2H), 6.92 (d, *J* = 9.0 Hz, 2H), 5.74 (s, 1H), 3.59 (d, *J* = 12.3 Hz, 2H), 2.67 – 2.55 (m, 2H), 2.28 – 2.22 (m, 2H), 1.97 – 1.87 (s, 1H), 1.85 – 1.80 (m, 2H), 1.70 – 1.68 (m, 2H), 1.61 – 1.56 (m, 2H), 1.50 – 1.46 (m, 2H), 1.27 – 1.21 (m, 2H), 0.94 (d, *J* = 6.5 Hz, 3H); Anal. Calcd for C₂₄H₂₈N₈O: C, 64.85; H, 6.35; N, 25.21;

Found: C, 64.79; H, 6.34; N, 25.19.

5-cyclopentyl-7-((4-(pyrrolidin-1-yl)phenyl)amino)-[1,2,4]triazolo[4,3-f]pteridin-4(5H)-one (H₆)

Yield: 66.1%; m.p.: 327.1 – 329.2 °C; MS (ESI) *m/z*: 415.4 [M-H]⁻; ¹H NMR (600 MHz, DMSO-*d*₆) δ 9.71 (s, 1H), 9.57 (s, 1H), 9.13 (s, 1H), 7.40 (d, *J* = 8.5 Hz, 2H), 6.53 (d, *J* = 8.9 Hz, 2H), 5.73 (s, 1H), 3.21 (t, *J* = 6.4 Hz, 4H), 2.28 – 3.22 (m, 2H), 1.96 – 1.94 (m, 4H), 1.93 – 1.88 (m, 2H), 1.82 – 1.81 (m, 2H), 1.59 – 1.55 (m, 2H); Anal. Calcd for C₂₂H₂₄N₈O: C, 63.45; H, 5.81; N, 26.90; Found: C, 63.44; H, 5.76; N, 26.88.

5-cyclopentyl-7-((4-(3,5-dimethylpiperazin-1-yl)phenyl)amino)-[1,2,4]triazolo[4,3-f]pteridin-4(5H)-one (H₇)

Yield: 63.2%; m.p.: 275.6 – 277.3 °C; MS (ESI) *m/z*: 460.5 [M+H]⁺; ¹H NMR (400 MHz, DMSO-*d*₆) δ 9.73 (s, 1H), 9.68 (s, 1H), 9.17 (s, 1H), 7.47 (d, *J* = 8.8 Hz, 2H), 6.91 (d, *J* = 9.0 Hz, 2H), 5.78 – 5.69 (m, 1H), 3.48 (d, *J* = 9.7 Hz, 2H), 2.92 – 2.84 (m, 2H), 2.28 – 2.20 (m, 2H), 2.11 (t, *J* = 10.9 Hz, 2H), 1.99 – 1.90 (m, 2H), 1.87 – 1.78 (m, 2H), 1.64 – 1.56 (m, 2H), 1.04 (d, *J* = 6.3 Hz, 6H); Anal. Calcd for C₂₄H₂₉N₉O: C, 62.73; H, 6.36; N, 27.43; Found: C, 62.71; H, 6.32; N, 27.40.

5-cyclopentyl-7-((4-thiomorpholinophenyl)amino)-[1,2,4]triazolo[4,3-f]pteridin-4(5H)-one (H₈)

Yield: 56.2%; m.p.: 310.6 – 312.3 °C; MS (ESI) *m/z*: 447.5 [M-H]⁻; ¹H NMR (400 MHz, DMSO-*d*₆) δ 9.72 (s, 2H), 9.17 (s, 1H), 7.50 (d, *J* = 8.9 Hz, 2H), 6.93 (d, *J* = 9.0 Hz, 2H), 5.76 – 5.72 (m, 1H), 3.46 – 3.43 (m, 4H), 2.70 – 2.68 (m, 4H), 2.28 – 2.23 (m, 2H), 1.94 – 1.90 (m, 2H), 1.85 – 1.79 (m, 2H), 1.64 – 1.58 (m, 2H); Anal. Calcd for C₂₂H₂₄N₈OS: C, 58.91; H, 5.39; N, 24.98; Found: C, 58.84; H, 5.36; N, 24.96.

5-cyclopentyl-7-((4-(4-(2-hydroxyethyl)piperazin-1-yl)phenyl)amino)-[1,2,4]triazolo[4,3-f]pteridin-4(5H)-one (H₉)

Yield: 44.6%; m.p.: 337.2 – 338.9 °C; MS (ESI) *m/z*: 476.6 [M+H]⁺; ¹H NMR (400 MHz, DMSO-*d*₆) δ 9.73 (s, 1H), 9.70 (s, 1H), 9.17 (s, 1H), 7.48 (d, *J* = 8.8 Hz, 2H), 6.92 (d, *J* = 9.0 Hz, 2H), 5.76 – 5.72 (m, 1H), 3.55 – 3.52 (m, 2H), 3.10 – 3.07 (m, 4H), 2.57 – 2.55 (m, 4H), 2.43 (t, *J* = 6.2 Hz, 2H), 2.45 – 2.42 (m, 2H), 1.92 (s, 2H), 1.85 (s, 2H), 1.64 – 1.56 (m, 2H); Anal. Calcd for C₂₄H₂₉N₉O₂: C, 60.62; H, 6.15; N, 26.51; Found: C, 60.59; H, 6.12; N, 26.45.

5-cyclopentyl-7-((4-(4-hydroxypiperidin-1-yl)phenyl)amino)-[1,2,4]triazolo[4,3-f]pteridin-4(5H)-one (H₁₀)

Yield: 61.9%; m.p.: 307.2 – 308.5 °C; MS (ESI) *m/z*: 445.6 [M-H]⁻; ¹H NMR (400 MHz, DMSO-*d*₆) δ 9.72 (s, 1H), 9.68 (s, 1H), 9.17 (s, 1H), 7.46 (d, *J* = 8.9 Hz, 2H), 6.92 (d, *J* = 9.0 Hz, 2H), 5.78 – 5.69 (m, 1H), 4.65 (d, *J* = 4.0 Hz, 1H), 3.63 – 3.58 (m, 1H), 3.51 – 3.45 (m, 2H), 3.17 (d, *J* = 4.7 Hz, 1H), 2.82 – 2.75 (m, 2H), 2.29 – 2.21 (m, 2H), 1.92 (s, 2H), 1.83 – 1.81 (m, 4H), 1.62 – 1.59 (m, 2H), 1.53 – 1.44 (m, 2H); Anal. Calcd for C₂₂H₂₅N₉O₂: C, 59.05; H, 5.63; N, 28.17; Found: C, 59.03; H, 5.61; N, 28.13.

5-cyclopentyl-7-((4-(cyclopentylamino)phenyl)amino)-[1,2,4]triazolo[4,3-f]pteridin-4(5H)-one (H₁₁)

Yield: 62.3%; m.p.: 291.2 – 292.3 °C; MS (ESI) *m/z*: 429.5 [M-H]⁻; ¹H NMR (400 MHz, DMSO-*d*₆) δ 9.71 (s, 1H), 9.48 (s, 1H), 9.13 (s, 1H), 7.27 (d, *J* = 8.6 Hz, 2H), 6.55 (d, *J* = 8.8 Hz, 2H), 5.72 – 5.68 (m, 1H), 5.38 (d, *J* = 6.5 Hz, 1H), 3.71 – 3.64 (m, 1H), 2.30 – 2.21 (m, 2H), 1.95 – 1.87 (m, 4H), 1.83 – 1.76 (m, 2H), 1.71 – 1.63 (m, 2H), 1.58 – 1.51 (m, 4H), 1.46 – 1.39 (m, 2H); Anal. Calcd for C₂₃H₂₆N₈O: C, 64.17; H, 6.09; N, 26.03; Found: C, 64.13; H, 6.05; N, 26.01.

5-cyclopentyl-7-((4-(dimethylamino)phenyl)amino)-[1,2,4]triazolo[4,3-f]pteridin-4(5H)-one (H₁₂)

Yield: 52.1%; m.p.: 311.2 – 313.3 °C; MS (ESI) m/z : 389.5 [M-H]⁻; ¹H NMR (400 MHz, DMSO-*d*₆) δ 9.72 (s, 1H), 9.61 (s, 1H), 9.15 (s, 1H), 7.43 (d, J = 8.9 Hz, 2H), 6.74 (d, J = 9.0 Hz, 2H), 5.75 – 5.71 (m, 1H), 2.87 (s, 6H), 2.39 – 2.20 (m, 2H), 1.96 – 1.89 (m, 2H), 1.86 – 1.78 (m, 2H), 1.62 – 1.55 (m, 2H); Anal. Calcd for C₂₀H₂₂N₈O: C, 61.52; H, 5.68; N, 28.70; Found: C, 61.46; H, 5.62; N, 28.67.

*5-cyclopentyl-7-((4-(4-cyclopentylpiperazin-1-yl)phenyl)amino)-[1,2,4]triazolo[4,3-*f*]pteridin-4(5*H*)-one (H₁₃)*

Yield: 66.2%; m.p.: 334.1 – 335.9 °C; MS (ESI) m/z : 500.7 [M+H]⁺; ¹H NMR (400 MHz, DMSO-*d*₆) δ 9.72 (s, 2H), 9.17 (s, 1H), 7.48 (d, J = 7.9 Hz, 2H), 6.92 (d, J = 8.3 Hz, 2H), 5.78 – 5.70 (m, 1H), 3.08 (s, 4H), 2.55 (s, 4H), 2.29 – 2.21 (m, 2H), 1.96 – 1.88 (m, 2H), 1.68 – 1.76 (m, 4H), 1.67 – 1.57 (m, 4H), 1.53 – 1.48 (m, 2H), 1.41 – 1.31 (m, 2H); Anal. Calcd for C₂₇H₃₃N₉O: C, 64.91; H, 6.66; N, 25.23; Found: C, 64.87; H, 6.62; N, 25.19.

*5-cyclopentyl-7-((4-(4-cyclopentylpiperazin-1-yl)phenyl)amino)-[1,2,4]triazolo[4,3-*f*]pteridin-4(5*H*)-one (H₁₄)*

Yield: 57.8%; m.p.: 320.0 – 322.1 °C; MS (ESI) m/z : 529.7 [M+H]⁺; ¹H NMR (400 MHz, DMSO-*d*₆) δ 9.73 (s, 1H), 9.70 (s, 1H), 9.17 (s, 1H), 7.46 (d, J = 8.9 Hz, 2H), 6.92 (d, J = 9.0 Hz, 2H), 5.76 – 5.72 (m, 1H), 3.65 (d, J = 12.4 Hz, 2H), 3.51 (s, 1H), 2.62 (t, J = 11.5 Hz, 2H), 2.35 – 2.21 (m, 7H), 2.14 (s, 3H), 2.04 – 1.78 (m, 8H), 1.64 – 1.57 (m, 2H), 1.54 – 1.45 (m, 3H); Anal. Calcd for C₂₈H₃₆N₁₀O: C, 63.61; H, 6.86; N, 26.50; Found: C, 63.58; H, 6.82; N, 26.48.

*5-cyclopentyl-7-((4-morpholinophenyl)amino)tetrazolo[1,5-*f*]pteridin-4(5*H*)-one (Y₁)*

Yield: 53.2%; m.p.: 303.1 – 306.2 °C; ¹H NMR (400 MHz, DMSO-*d*₆) δ 10.05 (s, 1H), 9.29 (s, 1H), 7.52 (d, J = 8.4 Hz, 2H), 6.97 (d, J = 8.9 Hz, 2H), 5.77 (s, 1H), 3.76 – 3.74 (m, 4H), 3.08 – 3.07 (m, 4H), 2.29 – 2.21 (m, 2H), 2.00 – 1.92 (m, 2H), 1.88 – 1.82 (m, 2H), 1.67 – 1.57 (m, 2H); Anal. Calcd for C₂₁H₂₃N₉O₂: C, 58.19; H, 5.35; N, 29.08; Found: C, 58.16; H, 5.30; N, 29.76.

*5-cyclopentyl-7-((4-(4-methylpiperazin-1-yl)phenyl)amino)tetrazolo[1,5-*f*]pteridin-4(5*H*)-one (Y₂)*

Yield: 58.0%; m.p.: 311.2 – 312.5 °C; MS (ESI) m/z : 445.4 [M-H]⁻; ¹H NMR (400 MHz, DMSO-*d*₆) δ 10.01 (s, 1H), 9.28 (s, 1H), 7.49 (d, J = 8.6 Hz, 2H), 6.95 (d, J = 9.0 Hz, 2H), 5.76 (s, 1H), 3.12 – 3.09 (m, 4H), 2.48 – 2.44 (m, 4H), 2.29 – 2.25 (m, 2H), 2.22 (s, 3H), 1.99 – 1.90 (m, 2H), 1.86 – 1.81 (m, 2H), 1.65 – 1.57 (m, 2H); Anal. Calcd for C₂₂H₂₆N₁₀O: C, 59.18; H, 5.87; N, 31.37. Found: C, 59.14; H, 5.82; N, 31.35.

*5-cyclopentyl-7-((4-(4-ethylpiperazin-1-yl)phenyl)amino)tetrazolo[1,5-*f*]pteridin-4(5*H*)-one (Y₃)*

Yield: 58.0%; m.p.: 324.8 – 325.9 °C; MS (ESI) m/z : 459.6 [M-H]⁻; ¹H NMR (400 MHz, DMSO-*d*₆) δ 10.00 (s, 1H), 9.27 (s, 1H), 7.49 (d, J = 8.4 Hz, 2H), 6.95 (d, J = 9.0 Hz, 2H), 5.76 (s, 1H), 3.12 – 3.09 (m, 4H), 2.37 (q, J = 7.1 Hz, 2H), 2.28 – 2.20 (m, 2H), 1.98 – 1.81 (m, 4H), 1.64 – 1.58 (m, 2H), 1.04 (t, J = 7.2 Hz, 3H); Anal. Calcd for C₂₂H₂₆N₁₀O: C, 59.18; H, 5.87; N, 31.37. Found: C, 59.14; H, 5.82; N, 31.35.

*5-cyclopentyl-7-((4-(piperidin-1-yl)phenyl)amino)tetrazolo[1,5-*f*]pteridin-4(5*H*)-one (Y₄)*

Yield: 61.2%; m.p.: 304.4 – 305.9 °C; ¹H NMR (400 MHz, DMSO-*d*₆) δ 9.98 (s, 1H), 9.27 (s, 1H), 7.47 (d, J = 8.6 Hz, 2H), 6.94 (d, J = 9.0 Hz, 2H), 5.75 (s, 1H), 3.10 – 3.08 (m, 4H), 2.29 – 2.21 (m, 2H), 1.96 – 1.81 (m, 4H), 1.66 – 1.60 (m, 6H), 1.55 – 1.53 (m, 2H); Anal. Calcd for C₂₂H₂₅N₉O: C, 61.24; H, 5.84; N, 29.21; Found: C, 61.21; H, 5.81; N, 29.16.

*5-cyclopentyl-7-((4-(4-methylpiperidin-1-yl)phenyl)amino)tetrazolo[1,5-*f*]pteridin-4(5*H*)-one (Y₅)*

Yield: 56.7%; m.p.: 250.1 – 252.3 °C; MS (ESI) m/z : 468.4 [M+Na]⁺; ¹H NMR (400 MHz, DMSO-*d*₆) δ 9.98 (s, 1H), 9.27 (s, 1H), 7.47 (d, J = 8.5 Hz, 2H), 6.94 (d, J = 9.0 Hz, 2H), 5.76 (s,

1H), 3.62 (d, $J = 12.2$ Hz, 2H), 2.62 (dd, $J = 12.2, 10.0$ Hz, 2H), 2.29 – 2.21 (m, 2H), 1.97 – 1.84 (m, 4H), 1.71 – 1.67 (m, 2H), 1.62 – 1.60 (m, 2H), 1.51 – 1.46 (m, 1H), 1.29 – 1.23 (m, 2H), 0.94 (d, $J = 6.5$ Hz, 3H); Anal. Calcd for $C_{23}H_{27}N_9O$: C, 62.01; H, 6.11; N, 28.30; Found: C, 61.93; H, 6.07; N, 28.29.

5-cyclopentyl-7-((4-(pyrrolidin-1-yl)phenyl)amino)tetrazolo[1,5-f]pteridin-4(5H)-one (Y₆)

Yield: 65.2%; m.p.: 288.7 – 290.9 °C; ¹H NMR (600 MHz, DMSO) δ 9.99 (s, 1H), 9.28 (s, 1H), 7.47 (d, $J = 7.2$ Hz, 2H), 6.94 (d, $J = 8.9$ Hz, 2H), 5.81 – 5.69 (m, 1H), 3.11 – 3.08 (m, 4H), 2.28 – 2.22 (m, 2H), 1.85 (s, 2H), 1.65 – 1.58 (m, 6H), 1.55 – 1.51 (m, 2H); Anal. Calcd for $C_{21}H_{23}N_9O$: C, 60.42; H, 5.55; N, 30.20; Found: C, 60.40; H, 5.51; N, 30.17.

5-cyclopentyl-7-((4-(3,5-dimethylpiperazin-1-yl)phenyl)amino)tetrazolo[1,5-f]pteridin-4(5H)-one (Y₇)

Yield: 66.0%; m.p.: 297.4 – 298.1 °C; MS (ESI) m/z : 461.5 [M+H]⁺; ¹H NMR (400 MHz, DMSO-*d*₆) δ 9.99 (s, 1H), 9.28 (s, 1H), 7.48 (d, $J = 8.4$ Hz, 2H), 6.94 (d, $J = 9.0$ Hz, 2H), 5.76 (s, 1H), 3.49 (d, $J = 9.6$ Hz, 2H), 2.89 – 2.84 (m, 2H), 2.27 – 2.20 (m, 2H), 2.10 (t, $J = 10.9$ Hz, 2H), 1.94 – 1.81 (m, 4H), 1.64 – 1.59 (m, 2H), 1.03 (d, $J = 6.3$ Hz, 6H); ¹³C NMR (101 MHz, DMSO) δ 159.11, 152.63, 149.67, 148.03, 147.74, 147.69, 143.33, 130.93, 122.34, 116.11, 56.03, 50.61, 40.63, 40.42, 40.21, 40.00, 39.79, 39.58, 39.37, 29.48, 28.03, 25.62, 19.79. Anal. Calcd for $C_{23}H_{28}N_{10}O$: C, 59.98; H, 6.13; N, 30.41; Found: C, 59.96; H, 6.10; N, 30.38.

5-cyclopentyl-7-((4-(3,5-dimethylpiperazin-1-yl)phenyl)amino)tetrazolo[1,5-f]pteridin-4(5H)-one (Y₈)

Yield: 43.9%; m.p.: 296.1 – 297.4 °C; MS (ESI) m/z : 448.5 [M-H]⁻; ¹H NMR (400 MHz, DMSO-*d*₆) δ 10.01 (s, 1H), 9.28 (s, 1H), 7.50 (d, $J = 8.5$ Hz, 2H), 6.95 (d, $J = 8.9$ Hz, 2H), 5.76 (s, 1H), 3.48 – 3.46 (m, 4H), 2.71 – 2.67 (m, 4H), 2.29 – 2.21 (m, 2H), 2.00 – 1.84 (m, 4H), 1.66 – 1.57 (m, 2H); Anal. Calcd for $C_{21}H_{23}N_9OS$: C, 56.11; H, 5.16; N, 28.04; Found: C, 56.08; H, 5.14; N, 28.03

5-cyclopentyl-7-((4-(4-(2-hydroxyethyl)piperazin-1-yl)phenyl)amino)tetrazolo[1,5-f]pteridin-4(5H)-one (Y₉)

Yield: 42.1%; m.p.: 344.6 – 345.6 °C; MS (ESI) m/z : 475.6 [M-H]⁻; ¹H NMR (400 MHz, DMSO-*d*₆) δ 9.99 (s, 1H), 9.27 (s, 1H), 7.49 (d, $J = 8.5$ Hz, 2H), 6.94 (d, $J = 9.0$ Hz, 2H), 5.75 (s, 1H), 4.42 (s, 1H), 3.55 – 3.50 (m, 2H), 3.11 – 3.09 (m, 4H), 2.57 – 2.55 (m, 4H), 2.44 (t, $J = 6.2$ Hz, 2H), 2.30 – 2.21 (m, 2H), 1.99 – 1.81 (m, 4H), 1.66 – 1.56 (m, 2H); Anal. Calcd for $C_{23}H_{28}N_{10}O_2$: C, 57.97; H, 5.92; N, 29.39; Found: C, 57.95; H, 5.89; N, 29.34

5-cyclopentyl-7-((4-(4-hydroxypiperidin-1-yl)phenyl)amino)tetrazolo[1,5-f]pteridin-4(5H)-one (Y₁₀)

Yield: 48.9%; m.p.: 312.5 – 313.8 °C; MS (ESI) m/z : 448.2 [M+H]⁺; ¹H NMR (400 MHz, DMSO-*d*₆) δ 9.98 (s, 1H), 9.27 (s, 1H), 7.47 (d, $J = 8.7$ Hz, 2H), 6.95 (d, $J = 9.0$ Hz, 2H), 5.75 (s, 1H), 4.66 (d, $J = 3.7$ Hz, 1H), 3.62 (s, 1H), 3.51 (s, 2H), 2.83 – 2.78 (m, 2H), 2.28 – 2.20 (m, 2H), 2.00 – 1.78 (m, 2H), 1.83 – 1.78 (m, 4H), 1.65 – 1.57 (m, 2H), 1.53 – 1.45 (m, 2H); Anal. Calcd for $C_{21}H_{24}N_{10}O_2$: C, 56.24; H, 5.39; N, 31.23; Found: C, 56.20; H, 5.36; N, 31.19

5-cyclopentyl-7-((4-(cyclopentylamino)phenyl)amino)tetrazolo[1,5-f]pteridin-4(5H)-one (Y₁₁)

Yield: 37.6%; m.p.: 324.4 – 325.1 °C; MS (ESI) m/z : 430.3 [M-H]⁻; ¹H NMR (400 MHz, DMSO-*d*₆) δ 9.79 (s, 1H), 9.22 (s, 1H), 7.28 (d, $J = 8.1$ Hz, 2H), 6.57 (d, $J = 8.7$ Hz, 2H), 5.75 (s, 1H), 5.45 (d, $J = 5.6$ Hz, 1H), 3.71 – 2.67 (m, 1H), 2.29 – 2.22 (m, 2H), 1.94 – 1.82 (m, 6H), 1.68 – 1.62 (m, 2H), 1.59 – 1.53 (m, 4H), 1.47 – 1.41 (m, 2H); Anal. Calcd for $C_{22}H_{25}N_9O$: C, 61.24; H,

5.84; N, 29.21; Found: C, 61.21; H, 5.80; N, 29.19.

5-cyclopentyl-7-((4-(dimethylamino)phenyl)amino)tetrazolo[1,5-f]pteridin-4(5H)-one (Y₁₂)

Yield: 52.3%; m.p.: 295.7 – 296.8 °C; MS (ESI) *m/z*: 392.4 [M+H]⁺; ¹H NMR (400 MHz, DMSO-*d*₆) δ 9.91 (s, 1H), 9.25 (s, 1H), 7.44 (d, *J* = 8.7 Hz, 2H), 6.75 (d, *J* = 9.0 Hz, 2H), 5.77 – 5.70 (m, 1H), 2.88 (s, 6H), 2.29 – 2.20 (m, 2H), 2.99 – 1.91 (m, 2H), 1.85 – 1.81 (m, 2H), 1.63 – 1.57 (m, 2H); Anal. Calcd for C₁₉H₂₁N₉O: C, 58.30; H, 5.41; N, 32.21; Found: C, 58.25; H, 5.36; N, 32.19.

5-cyclopentyl-7-((4-(4-cyclopentylpiperazin-1-yl)phenyl)amino)tetrazolo[1,5-f]pteridin-4(5H)-one (Y₁₃)

Yield: 55.6%; m.p.: 298.4 – 299.1 °C; MS (ESI) *m/z*: 501.7 [M+H]⁺; ¹H NMR (400 MHz, DMSO-*d*₆) δ 9.99 (s, 1H), 9.27 (s, 1H), 7.49 (d, *J* = 8.4 Hz, 2H), 6.94 (d, *J* = 8.9 Hz, 2H), 5.75 (s, 1H), 3.51 (s, 1H), 3.11 – 3.09 (m, 4H), 2.57 – 2.55 (m, 4H), 2.30 – 2.21 (m, 2H), 2.00 – 1.92 (m, 2H), 1.83 – 1.78 (m, 4H), 1.66 – 1.59 (m, 4H), 1.56 – 1.50 (m, 2H), 1.40 – 1.32 (m, 2H); Anal. Calcd for C₂₆H₃₂N₁₀O: C, 62.38; H, 6.44; N, 27.98; Found: C, 62.35; H, 6.41; N, 27.95

5-cyclopentyl-7-((4-(4-(4-methylpiperazin-1-yl)piperidin-1-yl)phenyl)amino)tetrazolo[1,5-f]pteridin-4(5H)-one (Y₁₄)

Yield: 61.3%; m.p.: 302.1 – 303.8 °C; MS (ESI) *m/z*: 530.7 [M+H]⁺; ¹H NMR (400 MHz, DMSO-*d*₆) δ 9.99 (s, 1H), 9.27 (s, 1H), 7.47 (d, *J* = 8.4 Hz, 2H), 6.95 (d, *J* = 9.0 Hz, 2H), 5.76 (s, 1H), 3.67 (d, *J* = 12.1 Hz, 2H), 3.51 (s, 1H), 2.63 (t, *J* = 11.3 Hz, 2H), 2.36 – 2.21 (m, 7H), 2.14 (s, 3H), 2.00 – 1.79 (m, 8H), 1.66 – 1.57 (s, 2H), 1.54 – 1.45 (m, 3H); Anal. Calcd for C₂₇H₃₅N₁₁O: C, 61.23; H, 6.66; N, 29.09; Found: C, 61.20; H, 6.63; N, 29.01

5-cyclopentyl-1-methyl-7-((4-morpholinophenyl)amino)-[1,2,4]triazolo[4,3-f]pteridin-4(5H)-one (L₁)

Yield: 49.8%; m.p.: 306.2 – 304.9 °C; MS (ESI) *m/z*: 447.7 [M+H]⁺; ¹H NMR (400 MHz, DMSO-*d*₆) δ 9.70 (s, 1H), 8.98 (s, 1H), 7.53 (d, *J* = 8.8 Hz, 2H), 6.93 (d, *J* = 9.0 Hz, 2H), 5.79 – 5.74 (m, 1H), 3.76 – 3.73 (m, 4H), 3.07 – 3.05 (m, 4H), 2.92 (s, 3H), 2.29 – 2.20 (m, 2H), 1.99 – 1.91 (m, 2H), 1.88 – 1.80 (m, 2H), 1.64 – 1.57 (m, 2H); Anal. Calcd for C₂₃H₂₆N₈O₂: C, 61.87; H, 5.87; N, 25.10; Found: C, 61.84; H, 5.82; N, 25.07.

5-cyclopentyl-1-methyl-7-((4-(4-methylpiperazin-1-yl)phenyl)amino)-[1,2,4]triazolo[4,3-f]pteridin-4(5H)-one (L₂)

Yield: 56.4%; m.p.: 296.6 – 297.3 °C; MS (ESI) *m/z*: 460.6 [M+H]⁺; ¹H NMR (400 MHz, DMSO-*d*₆) δ 9.67 (s, 1H), 8.98 (s, 1H), 7.50 (d, *J* = 8.7 Hz, 2H), 6.92 (d, *J* = 9.0 Hz, 2H), 5.79 – 5.74 (m, 1H), 3.09 – 3.07 (m, 4H), 2.92 (s, 3H), 2.47 – 2.44 (m, 4H), 2.28 – 2.24 (m, 2H), 2.22 (s, 3H), 1.98 – 1.91 (m, 2H), 1.87 – 1.80 (m, 2H), 1.64 – 1.56 (m, 2H); Anal. Calcd for C₂₄H₂₉N₉O: C, 62.73; H, 6.36; N, 27.43; Found: C, 62.69; H, 6.31; N, 27.40.

5-cyclopentyl-7-((4-(4-ethylpiperazin-1-yl)phenyl)amino)-1-methyl-[1,2,4]triazolo[4,3-f]pteridin-4(5H)-one (L₃)

Yield: 53.0%; m.p.: 299.6 – 302.2 °C; MS (ESI) *m/z*: 474.7 [M+H]⁺; ¹H NMR (400 MHz, DMSO-*d*₆) δ 9.68 (s, 1H), 8.97 (s, 1H), 7.50 (d, *J* = 8.7 Hz, 2H), 6.92 (d, *J* = 9.0 Hz, 2H), 5.78 – 5.75 (m, 1H), 3.10 – 3.08 (m, 4H), 2.92 (s, 3H), 2.37 (q, *J* = 7.1 Hz, 2H), 2.28 – 2.20 (m, 2H), 1.98 – 1.89 (m, 2H), 1.87 – 1.79 (m, 2H), 1.64 – 1.56 (m, 2H), 1.03 (t, *J* = 7.2 Hz, 3H); ¹³C NMR (101 MHz, DMSO-*d*₆) δ 157.48, 153.26, 149.43, 148.66, 147.54, 146.75, 143.66, 131.86, 121.81, 116.13, 110.19, 53.89, 52.84, 52.11, 49.27, 40.61, 40.40, 40.19, 39.98, 39.78, 39.57, 39.36, 28.14, 25.59, 14.25, 12.45; Anal. Calcd for C₂₅H₃₁N₉O: C, 63.40; H, 6.60; N, 26.62; Found: C, 63.37; H, 6.58; N,

26.59.

5-cyclopentyl-1-methyl-7-((4-(piperidin-1-yl)phenyl)amino)-[1,2,4]triazolo[4,3-f]pteridin-4(5H)-one (L₄)

Yield: 62.4%; m.p.: 325.8 – 327.9 °C; MS (ESI) m/z : 445.6 [M+H]⁺; ¹H NMR (400 MHz, DMSO-*d*₆) δ 9.66 (s, 1H), 8.97 (s, 1H), 7.48 (d, J = 8.8 Hz, 2H), 6.91 (d, J = 9.0 Hz, 2H), 5.87 – 5.64 (m, 1H), 3.13 – 3.02 (m, 4H), 2.92 (s, 3H), 2.29 – 2.19 (m, 2H), 1.93 (s, 2H), 1.89 – 1.78 (m, 2H), 1.66 – 1.58 (m, 6H), 1.55 – 1.50 (m, 2H); Anal. Calcd for C₂₄H₂₈N₈O: C, 64.85; H, 6.35; N, 25.21; Found: C, 64.83; H, 6.33; N, 25.19.

5-cyclopentyl-1-methyl-7-((4-(4-methylpiperidin-1-yl)phenyl)amino)-[1,2,4]triazolo[4,3-f]pteridin-4(5H)-one (L₅)

Yield: 67.8%; m.p.: 308.7 – 309.6 °C; MS (ESI) m/z : 457.6 [M-H]⁻; ¹H NMR (400 MHz, DMSO-*d*₆) δ 9.66 (s, 1H), 8.97 (s, 1H), 7.47 (d, J = 8.7 Hz, 2H), 6.91 (d, J = 9.0 Hz, 2H), 5.77 – 5.74 (m, 1H), 3.59 (d, J = 12.2 Hz, 2H), 2.92 (s, 3H), 2.60 (t, J = 11.2 Hz, 2H), 2.29 – 2.20 (m, 2H), 1.93 (s, 2H), 1.86 – 1.80 (m, 2H), 1.69 (d, J = 12.3 Hz, 2H), 1.61 – 1.57 (m, 2H), 1.52 – 1.44 (m, 1H), 1.28 – 1.23 (m, 2H), 0.94 (d, J = 6.5 Hz, 3H); Anal. Calcd for C₂₅H₃₀N₈O: C, 65.48; H, 6.59; N, 24.44; Found: C, 65.46; H, 6.57; N, 24.42.

5-cyclopentyl-1-methyl-7-((4-(pyrrolidin-1-yl)phenyl)amino)-[1,2,4]triazolo[4,3-f]pteridin-4(5H)-one (L₆)

Yield: 55.7%; m.p.: 315.4 – 316.8 °C; MS (ESI) m/z : 431.5 [M+H]⁺; ¹H NMR (400 MHz, DMSO-*d*₆) δ 9.54 (s, 1H), 8.94 (s, 1H), 7.41 (d, J = 8.4 Hz, 2H), 6.52 (d, J = 8.7 Hz, 2H), 5.79 – 5.72 (m, 1H), 3.21-3.19 (m, 4H), 2.91 (s, 3H), 2.28 – 2.18 (m, 2H), 1.99 – 1.88 (m, 6H), 1.85 – 1.77 (m, 2H), 1.62 – 1.54 (m, 2H); Anal. Calcd for C₂₃H₂₆N₈O: C, 64.17; H, 6.09; N, 26.03; Found: C, 64.15; H, 6.08; N, 26.01.

5-cyclopentyl-7-((4-(3,5-dimethylpiperazin-1-yl)phenyl)amino)-1-methyl-[1,2,4]triazolo[4,3-f]pteridin-4(5H)-one (L₇)

Yield: 53.2%; m.p.: 280.4 – 282.1 °C; MS (ESI) m/z : 474.5 [M+H]⁺; ¹H NMR (400 MHz, DMSO-*d*₆) δ 9.64 (s, 1H), 8.97 (s, 1H), 7.48 (d, J = 8.7 Hz, 2H), 6.90 (d, J = 8.9 Hz, 2H), 5.78 – 5.74 (m, 1H), 3.46 (d, J = 9.6 Hz, 2H), 2.92 (s, 3H), 2.88 – 2.83 (m, 2H), 2.26 – 2.19 (m, 2H), 2.08 (t, J = 10.8 Hz, 2H), 1.96 – 1.89 (m, 2H), 1.87 – 1.79 (m, 2H), 1.64 – 1.56 (m, 2H), 1.02 (d, J = 6.2 Hz, 6H); ¹³C NMR (101 MHz, DMSO) δ 157.51, 153.27, 149.43, 148.65, 147.68, 146.78, 143.67, 131.58, 121.88, 116.15, 110.15, 56.31, 53.87, 50.61, 40.63, 40.42, 40.22, 40.01, 39.80, 39.59, 39.38, 28.17, 25.63, 19.91, 14.25; Anal. Calcd for C₂₅H₃₁N₉O: C, 63.40; H, 6.60; N, 26.62; Found: C, 63.38; H, 6.57; N, 26.56.

5-cyclopentyl-1-methyl-7-((4-thiomorpholinophenyl)amino)-[1,2,4]triazolo[4,3-f]pteridin-4(5H)-one (L₈)

Yield: 64.3%; m.p.: 312.0 – 314.6 °C; MS (ESI) m/z : 461.6 [M-H]⁻; ¹H NMR (400 MHz, DMSO-*d*₆) δ 9.68 (s, 1H), 8.98 (s, 1H), 7.51 (d, J = 8.8 Hz, 2H), 6.92 (d, J = 9.0 Hz, 2H), 5.79 – 5.74 (m, 1H), 3.45 – 3.43 (m, 4H), 2.92 (s, 3H), 2.70 – 2.68 (m, 4H), 2.27 – 2.21 (m, 2H), 1.93 (s, 2H), 1.85 – 1.83 (m, 2H), 1.62 – 1.59 (m, 2H); Anal. Calcd for C₂₃H₂₆N₈OS: C, 59.72; H, 5.67; N, 24.22; Found: C, 59.69; H, 5.62; N, 24.18.

5-cyclopentyl-7-((4-(4-(2-hydroxyethyl)piperazin-1-yl)phenyl)amino)-1-methyl-[1,2,4]triazolo[4,3-f]pteridin-4(5H)-one (L₉)

Yield: 58.5%; m.p.: 288.4 – 289.9 °C; MS (ESI) m/z : 490.7 [M+H]⁺; ¹H NMR (400 MHz, DMSO-*d*₆) δ 9.66 (s, 1H), 8.97 (s, 1H), 7.49 (d, J = 8.8 Hz, 2H), 6.91 (d, J = 9.0 Hz, 2H), 5.81 –

5.71 (m, 1H), 4.41 (s, 1H), 3.57 – 3.51 (s, 2H), 3.09 – 3.07 (m, 4H), 2.92 (s, 3H), 2.57 – 2.55 (m, 4H), 2.44 (t, $J = 6.2$ Hz, 2H), 2.28 – 2.20 (m, 2H), 1.95 – 1.89 (m, 2H), 1.87 – 1.81 (m, 2H), 1.64 – 1.56 (m, 2H); Anal. Calcd for $C_{25}H_{31}N_9O_2$: C, 61.33; H, 6.38; N, 25.75; Found: C, 61.29; H, 6.35; N, 25.66.

5-cyclopentyl-7-((4-(4-hydroxypiperidin-1-yl)phenyl)amino)-1-methyl-[1,2,4]triazolo[4,3-f]pteridin-4(5H)-one (L₁₀)

Yield: 56.1%; m.p.: 321.2 – 323.8 °C; MS (ESI) m/z : 461.5 $[M+H]^+$; 1H NMR (400 MHz, DMSO- d_6) δ 9.65 (s, 1H), 8.97 (s, 1H), 7.48 (d, $J = 8.8$ Hz, 2H), 6.92 (d, $J = 9.0$ Hz, 2H), 5.78 – 5.74 (m, 1H), 4.65 (d, $J = 4.1$ Hz, 1H), 3.62 – 3.58 (m, 1H), 3.51–3.44 (m, 2H), 2.92 (s, 3H), 2.82 – 2.73 (m, 2H), 2.28–2.20 (m, 2H), 1.93 (s, 2H), 1.84 – 1.81 (m, 4H), 1.61 – 1.59 (m, 2H), 1.52 – 1.44 (m, 2H); Anal. Calcd for $C_{23}H_{27}N_9O_2$: C, 59.86; H, 5.90; N, 27.31; Found: C, 59.82; H, 5.87; N, 27.26.

5-cyclopentyl-7-((4-(cyclopentylamino)phenyl)amino)-1-methyl-[1,2,4]triazolo[4,3-f]pteridin-4(5H)-one (L₁₁)

Yield: 49.2%; m.p.: 312.6 – 314.2 °C; MS (ESI) m/z : 443.6 $[M-H]^-$; 1H NMR (400 MHz, DMSO- d_6) δ 9.45 (s, 1H), 8.93 (s, 1H), 7.28 (d, $J = 8.5$ Hz, 2H), 6.55 (d, $J = 8.8$ Hz, 2H), 5.73 (s, 1H), 5.38 (d, $J = 6.5$ Hz, 1H), 3.68 (dd, $J = 11.8, 5.6$ Hz, 1H), 2.91 (s, 3H), 2.23 – 2.21 (m, 2H), 1.92 – 1.87 (m, 4H), 1.84 – 1.77 (m, 2H), 1.69 – 1.63 (m, 2H), 1.58 – 1.56 (m, 4H), 1.46 – 1.41 (m, 2H); Anal. Calcd for $C_{24}H_{28}N_8O$: C, 64.85; H, 6.35; N, 25.21; Found: C, 64.83; H, 6.30; N, 25.18.

5-cyclopentyl-7-((4-(dimethylamino)phenyl)amino)-1-methyl-[1,2,4]triazolo[4,3-f]pteridin-4(5H)-one (L₁₂)

Yield: 64.3%; m.p.: 337.2 – 338.9 °C; MS (ESI) m/z : 403.5 $[M-H]^-$; 1H NMR (400 MHz, DMSO- d_6) δ 9.79 – 9.36 (m, 1H), 8.96 (s, 1H), 7.45 (d, $J = 8.8$ Hz, 2H), 6.73 (d, $J = 9.1$ Hz, 2H), 5.82 – 5.71 (m, 1H), 2.92 (s, 3H), 2.87 (s, 6H), 2.28 – 2.20 (m, 2H), 1.96 – 1.89 (m, 2H), 1.86 – 1.78 (m, 2H), 1.62 – 1.55 (m, 2H); Anal. Calcd for $C_{21}H_{24}N_8O$: C, 62.36; H, 5.98; N, 27.70; Found: C, 62.34; H, 5.93; N, 27.65.

5-cyclopentyl-7-((4-(4-cyclopentylpiperazin-1-yl)phenyl)amino)-1-methyl-[1,2,4]triazolo[4,3-f]pteridin-4(5H)-one (L₁₃)

Yield: 67.8%; m.p.: 331.4 – 334.6 °C; MS (ESI) m/z : 514.7 $[M+H]^+$; 1H NMR (400 MHz, DMSO- d_6) δ 9.67 (s, 1H), 8.97 (s, 1H), 7.50 (d, $J = 8.8$ Hz, 2H), 6.91 (d, $J = 9.0$ Hz, 2H), 5.81 – 5.73 (m, 1H), 3.09 – 3.07 (m, 4H), 2.92 (s, 3H), 2.56 – 2.54 (m, 4H), 2.28 – 2.20 (m, 2H), 1.93 (s, 2H), 1.86 – 1.78 (m, 4H), 1.65 – 1.56 (m, 4H), 1.53 – 1.50 (m, 2H), 1.40 – 1.33 (m, 2H); Anal. Calcd for $C_{28}H_{35}N_9O$: C, 65.47; H, 6.87; N, 24.54; Found: C, 65.42; H, 6.86; N, 24.51.

5-cyclopentyl-1-methyl-7-((4-(4-(4-methylpiperazin-1-yl)piperidin-1-yl)phenyl)amino)-[1,2,4]triazolo[4,3-f]pteridin-4(5H)-one (L₁₄)

Yield: 57.4%; m.p.: 327.9 – 329.5 °C; MS (ESI) m/z : 543.8 $[M+H]^+$; 1H NMR (400 MHz, DMSO- d_6) δ 9.67 (s, 1H), 8.97 (s, 1H), 7.50 (d, $J = 8.8$ Hz, 2H), 6.91 (d, $J = 9.0$ Hz, 2H), 5.80 – 5.72 (m, 1H), δ 3.65 (d, $J = 11.4$ Hz, 1H), 3.51 (s, 1H), 2.92 (s, 3H), 2.64 – 2.59 (m, 2H), 2.35 – 2.20 (m, 7H), 2.14 (s, 3H), 1.99 – 1.78 (m, 8H), 1.64 – 1.57 (m, 2H), 1.55 – 1.43 (m, 3H); Anal. Calcd for $C_{29}H_{38}N_{10}O$: C, 64.18; H, 7.06; N, 25.81; Found: C, 64.13; H, 7.02; N, 25.77.

4.1.5

N-(5-cyclopentyl-1-methyl-4-oxo-4,5-dihydro-[1,2,4]triazolo[4,3-f]pteridin-7-yl)-N-(4-(4-ethylpiperazin-1-yl)phenyl)acetamide (L₁₅)

The compound **L₃** (0.5 g, 0.9 mmol) was taken into acetic anhydride and stirred at 100 °C for 4 h.

The reaction mixture was cooled to room temperature, and the crude product was filtered. The pure product **L**₁₅ was obtained by flash column chromatography using dichloromethane/methanol as eluent.

Yield: 60.0%; m.p.: 331.2 – 333.6 °C; MS (ESI) *m/z*: 516.3 [M+H]⁺; ¹H NMR (600 MHz, DMSO-*d*₆) δ 9.25 (s, 1H), 7.10 (d, *J* = 8.8 Hz, 2H), 6.98 (d, *J* = 8.8 Hz, 2H), 5.54 – 5.48 (m, 1H), 3.16 – 3.15 (m, 4H), 2.95 (s, 3H), 2.36 (q, *J* = 7.1 Hz, 2H), 2.27 (s, 3H), 2.11 – 2.05 (m, 2H), 1.81 – 1.75 (m, 2H), 1.71 (s, 2H), 1.55 – 1.49 (m, 2H), 1.03 (t, *J* = 7.2 Hz, 3H). Anal. Calcd for C₂₇H₃₃N₉O₂: C, 62.89; H, 6.45; N, 24.45; Found: C, 62.77; H, 6.35; N, 24.23.

4.2 Biological section

4.2.1 MTT assay

MTT assay was carried out on A549, PC-3, HCT116, MCF-7, MDA-MB321 cells to evaluate antiproliferative activity of the target compounds. The cancer cell lines were cultured in minimum essential medium (MEM) supplement with 10% foetal bovine serum (FBS).

Approximate 5×10³ cells, suspended in MEM medium, were plated in a 96-well plate and incubated in 5% CO₂ at 37 °C for 24 h. The tested compounds were added to the culture medium and the cell cultures were incubated for another 72 h. The cells were incubated at 37 °C for 4 h with 10 μL of 5 mg/mL MTT solution. The formazan crystals in each well were dissolved in 100 μL dimethyl sulfoxide, and their absorbance were measured at 492 nm (absorbance of MTT formazan) and 630 nm (reference wave length) with an ELISA reader. The results, expressed as IC₅₀, are averages of at least three determinations and calculated using the Bacus Laboratories Incorporated Slide Scanner (Bliss) software.

4.2.2 In vitro enzyme assay

Enzymatic activity assay against CDK6 (Carna) and PLK1 (Millipore) was carried out by a well-established mobility shift assay. The kinase base buffer was consist of 20 mM HEPES (pH 7.5), 0.01% Triton X-100, 10 mM MgCl₂, and 2 mM DTT. The stop buffer contained a mixture of 100 mM HEPES (pH 7.5), 0.015% Brij-35, 0.2% Coating Reagent and 50 mM EDTA.

Initially, the tested compounds were diluted to 50-fold of the desired highest concentration in reaction by 100% DMSO. The tested compound dilution (100 μL) was transferred into a well in 96-well plate. Then, the controls were formed by adding 100 μL of 100% DMSO to two empty wells, which was marked as source plate. The intermediate plate was prepared by transferring 10 μL of compound from source plate to a new 96-well plate. In the intermediate plate, additional 90 μL of kinase buffer was added to each well. The intermediate plate was swayed for 10 min. Then, transferring 5 μL of each well from the 96-well intermediate plate to a 384-well plate in duplicates as the assay plate. In the each well of 384-well assay plate, the prepared enzyme solution (appropriate kinase in kinase base buffer) was added. The plate was then incubated at room temperature for 10 min. After that, the addition 10 μL of prepared peptide solution (FAM-labeled peptide and ATP in kinase base buffer) was added. The sample was incubated at 28 °C for 1 h, then 25 μL of stop buffer was added. The conversion data was copied from Caliper program, and the values were converted to inhibition values. Percent inhibition = (max - conversion)/ (max - min) × 100.

4.2.3 Morphology assays of apoptotic cells

Apoptotic morphological changes of A549 cells were detected by AO/EB staining. Briefly, A549 cells were seeded in six-well plates (5×10⁴/well) and then treated with different concentrations of **Y**₇ and **L**₇ for 24 h. The cells were washed with phosphate buffer saline (PBS)

and then stained with AO/EB mixed solution (AO: EB = 1: 1) for 15 min. The stained cells were washed twice with PBS and observed by fluorescence microscope (Olympus, Tokyo, Japan).

4.2.4 Cell migration assay

Cell migration assay were carried out using wound-healing assay. A549 cells were seeded in six-well plates (5×10^4 /well) and were allowed to grow to 100% confluence. A linear wound was made by a pipet tips across the confluent cell layer. A549 cells were washed twice with PBS, and then incubated with culture medium containing DMSO or different concentrations of compound **L**₇. After treatment for 12, 24 and 36 h, the images were taken by fluorescence microscope (Olympus, Tokyo, Japan).

4.2.5 Cell cycle distribution analysis

The effects of compound **L**₇ on cell cycle progression were confirmed by a standard propidium iodide (PI) staining procedure followed by flow cytometry analysis. Briefly, A549 cells were seeded in six-well plates (5×10^4 /well) and then treated with different concentrations of **L**₇ for 24 h. The cells were collected and washed twice with ice cold PBS, then immobilized in 70% ice cold ethanol overnight at 4 °C. The cells were washed again by PBS, and then the cell DNA was stained with PI (50 µg/mL) for 10 min. FL-2 signal was acquired and analysed using a flow cytometer.

4.3 Molecular docking

Structural alignment was accomplished through the Cresset Forge v10.4.1. The CDK6 or PLK1 models was built using PDB code: 5L2I and PDB code: 3FC2 as templates, respectively. The protein coordinates were downloaded from the Protein Data Bank (<http://www.rcsb.org/pdb/>). And palbociclib (PDB code: 5L2I), BI6727 (PDB code: 3FC2) are regarded as reference molecules for the computation of field points and alignment. The MCS conformations of the molecules in training set were generated by being aligned on the reference molecule. After the conformations were obtained, the highest structural arrangement score was recommended as the best alignment. Molecular field points are computed for the test set of molecules, together with the molecular field points of the training set structure were revealed to be the best alignment with the template field points. The analysis of results implemented on discovery studio visualizer software [33].

Acknowledgements

The work was financially supported by the Program for Innovative Research Team of the Ministry of Education and Program for Liaoning Innovative Research Team in University, the National Natural Science Foundation of China (Grant No. 81628012), the Fund for long-term training of young teachers in Shenyang Pharmaceutical University (ZQN2015002), the National Natural Science Foundation of Liaoning province (Grant No. 20170540854) and Training Program Foundation for the Distinguished Young Scholars of University in Liaoning Province (LJQ2015109).

References

- [1] R.L. Siegel, K.D. Miller, A. Jemal, Cancer statistics, 2016, CA: a cancer journal for Clinicians 66 (2016) 7–30.
- [2]<http://www.healthdata.org/news-release/cancer's-deadly-toll-grows-less-developed-countries-new-cases-increase-globally>.
- [3] H. Nagai, Y.H. Kim, Cancer prevention from the perspective of global cancer burden patterns, J. Thorac. Dis. 9 (2017) 448–451.
- [4] W.B. Kuang, R.Z. Huang, J.L. Qi, X. Lu, Q.P. Qin, B.Q. Zou, Z.F. Chen, H. Liang, Y. Zhang,

- Design, synthesis and pharmacological evaluation of new 3-(1Hbenzimidazol-2-yl)quinolin-2(1H)-one derivatives as potential antitumor agents, *Eur. J. Med. Chem.* 157 (2018) 139–150.
- [5] J. Akhtar, A.A. Khan, Z. Ali, R. Haider, M.Y. Shahar, Structure-activity relationship (SAR) study and design strategies of nitrogen-containing heterocyclic moieties for their anticancer activities, *Eur. J. Med. Chem.* 125 (2017) 143–189.
- [6] D. Rudolph, M. Steegmaier, M. Hoffmann, M. Grauert, A. Baum, J. Quant, C. Haslinger, P. Garin-Chesa, G.R. Adolf, BI 6727, A polo-like kinase inhibitor with improved pharmacokinetic profile and broad antitumor activity, *Clin. Cancer Res.* 15 (2009) 3094–3102.
- [7] Y.J. Hao, X. Wang, T. Zhang, D.H. Sun, Y. Tong, Y.Q. Xu, H.Y. Chen, L.J. Tong, L.L. Zhu, Z.J. Zhao, Z. Chen, J. Ding, H. Xie, Y.F. Xu, H.L. Li, Discovery and structural optimization of N5-substituted 6,7-dioxo-6,7-dihydropteridines as potent and selective epidermal growth factor receptor (EGFR) inhibitors against L858R/T790M resistance mutation, *J. Med. Chem.* 59 (2016) 7111–7124.
- [8] E. Christian, G. Kai, H. Niklas, W. Alexander, G. Ulrike, Preparation of spiroheterocycl-dihydropteridinones as modulators of γ -secretase for treating Alzheimer's disease, WO2014127816.
- [9] W. Ellen, T. Elizabeth, H. David, B. Benjamin, K. Stefan, C. Louis, H. Swen, Design and synthesis of dual ALK/BRD4 inhibitors, 255th ACS National Meeting & Exposition, New Orleans, LA, United States, March 18-22, 2018.
- [10] P. L. Toogood, P.J. Harvey, J.T. Repine, D.J. Sheehan, S.N. VanderWel, H. Zhou, P.R. Keller, D.J. McNamara, D. Sherry, T. Zhu, J. Brodfuehrer, C. Choi, M.R. Barvian, D.W. Fry, Discovery of a potent and selective inhibitor of cyclin-dependent kinase 4/6, *J. Med. Chem.* 48 (2005) 2388–2406.
- [11] V. Erik, Brameld, K. Albert, Preparation of quinolone derivatives as fibroblast growth factor receptor inhibitors, WO 2015120049.
- [12] H.M. Cheng, S. Bagrodia, S. Bailey, M. Edwards, J. Hoffman, Q.Y. Hu, R. Kania, D.R. Knighton, M.A. Marx, S. Ninkovic, S.X. Sun, E. Zhang, Discovery of the highly potent PI3K /mTOR dual inhibitor PF-04691502 through structure based drug design, *Med. Chem. Commun.* 1 (2010) 139–144.
- [13] D.M. Goldstein, M. Soth, T. Gabriel, N. Dewdney, A. Kuglstatler, H. Arzeno, J. Chen, W. Bingenheimer, S.A. Dalrymple, J. Dunn, R. Farrell, S. Frauchiger, J.L. Fargue, M. Ghate, B. Graves, R.J. Hill, F. Li, R. Litman, B. Loe, J. McIntosh, D. McWeeney, E. Papp, J. Park, H.F. Reese, R.T. Roberts, D. Rotstein, B.S. Pablo, K. Sarma, M. Stahl, M.L. Sung, R.T. Suttman, E.B. Sjogren, Y. Tan, A. Trejo, M. Welch, P. Weller, B.R. Wong, H. Zecic. Discovery of 6-(2,4-difluorophenoxy)-2-[3-hydroxy-1-(2-hydroxyethyl)propylamino]-8-methyl-8H-pyrido[2,3-d]pyrimidin-7-one (pamapimod) and 6-(2,4-difluorophenoxy)-8-methyl-2-(tetrahydro-2H-pyran-4-ylamino)pyrido[2,3-d]pyrimidin-7(8H)-one (R1487) as orally bioavailable and highly selective inhibitors of p38 α mitogen-activated protein kinase, *J. Med. Chem.* 54 (2011) 2255–2265.
- [14] P. Chen, N.V. Lee, W.Y. Hu, M.R. Xu, R.A. Ferre, H. Lam, S. Bergqvist, J. Solowiej, W. Diehl, Y.A. He, X. Yu, A. Nagata, T. VanArsdale, B.W. Murray, Spectrum and degree of CDK drug interactions predicts clinical performance, *Mol. Cancer Ther.* 15 (2016) 2273–2281.
- [15] a) P. Kumar, E.E. Knaus, Synthesis and antiinflammatory activity of

- 5-(1,6-dihydropyridyl)tetrazole-2-acetic acids, esters and amides, *Drug Des. Discov.* 11 (1994) 15–22; b) S. Shafi, M.M. Alam, N. Mulakayala, C. Mulakayala, G. Vanaja, A.M. Kalle, R. Pallud, M.S. Alam, Synthesis of novel 2-mercapto benzothiazole and 1,2,3-triazole based bis-heterocycles: Their anti-inflammatory and anti-nociceptive activities, *Eur. J. Med. Chem.* 49 (2012) 324–333.
- [16] J.S. Shukla, S. Saxena, Studies on substituted tetrazoles as CNS depressant, anticonvulsant and monoamine oxidase inhibitory agents, *Indian Drugs*, 18 (1980) 15–21.
- [17] a) O.H. Ko, H.R. Kang, J.C. Yoo, G.S. Kim, S.S. Hong, Synthesis and antimicrobial activity of cephalosporin antibiotic derivatives, *Yakhak Hoechi*, 36 (1992) 150–153; b) T.H. Fu, Y. Li, H.D. Thaker, R.W. Scott, G.N. Tew, Expedient synthesis of SMAMPs *via* click chemistry, *ACS Med. Chem. Lett.* 4 (2013) 841.
- [18] N. Dereu, M. Evers, C. Poujade, F. Soler, *PCT Int. Appl.* Preparation of lupane antiviral agents, WO 9426725.
- [19] H. Singh, K.K. Bhutani, R.K. Malhotra, D. Paul, Steroids and related studies. Part 49. 7a-Aza-B-homo[7a,7-d]tetrazole analogs of progesterone and testosterone, *J. Chem. Soc. Perkin Trans. I*, 12, (1979) 3166–3170.
- [20] a) H. Elamari, R. Slimi, G.G. Chabot, L. Quentin, D. Scherman, C. Girard. Synthesis and *in vitro* evaluation of potential anticancer activity of mono- and bis-1,2,3-triazole derivatives of bis-alkynes, *Eur. J. Med. Chem.* 60 (2013) 360–364; b) W.T. Li, W.H. Wu, C.H. Tang, R. Tai, S.T. Chen. One-pot tandem copper-catalyzed library synthesis of 1-thiazolyl-1,2,3-triazoles as anticancer agents, *ACS Comb. Sci.* 13 (2011) 72–78; c) A. Srivastava, L. Aggarwal, N. Jain, One-pot sequential alkynylation and cycloaddition: regioselective construction and biological evaluation of novel benzoxazole-triazole derivatives, *ACS Comb. Sci.* 17 (2015) 39–48.
- [21] M. Shekarchi, M.B. Marvasti, M. Sharifzadeh, A. Shafiee, Anticonvulsant activities of 7-phenyl-5H-thiazolo[5,4-e][1,2,3,4]tetrazolo[5,1-c]pyrrolo[1,2-a][1,4]diazepine and 7-phenyl-5H-thiazolo[5,4-e][1,3,4]triazolo[5,1-c]pyrrolo[1,2-a][1,4] diazepines, *Iran. J. Pharm. Res.* 4 (2005) 33–36.
- [22] M.M. Zhan, Y. Yang, J.F. Luo, X.X. Zhang, X. Xiao, S.Y. Li, K. Cheng, Z.L. Xie, Z.C. Tu, C.Z. Liao, Design, synthesis, and biological evaluation of novel highly selective polo-like kinase 2 inhibitors based on the tetrahydropteridin chemical scaffold, *Eur. J. Med. Chem.* 143 (2018) 724–731.
- [23] A. Kiryanov, S. Natala, B. Jones, C. McBride, V. Feher, B. Lam, Y. Liu, K. Hond, N. Uchiyama, T. Kawamoto, Y. Hikichi, L. Zhang, D. Hosfield, R. Skene, H. Zou, J. Stafford, X.D. Cao, T. Ichikawa, Structure-based design and SAR development of 5,6-dihydroimidazo[1,5-f]pteridine derivatives as novel Polo-like kinase-1 inhibitors, *Bioorg. Med. Chem. Lett.* 27 (2017) 1311–1315.
- [24] Y.T. Li, X.H. Luo, Q.X. Guo, Y.W. Nie, T.Q. Wang, C. Zhang, Z. Huang, X. Wang, Y.H. Liu, Y.N. Chen, J.Y. Zheng, S.Y. Yang, Y. Fan, R. Xiang, Discovery of *N*1-(4-((7-cyclopentyl-6-(dimethylcarbamoyl)-7H-pyrrolo[2,3-d]pyrimidin-2-yl)amino)phenyl)-*N*-8-hydroxyoctanediamide as a novel inhibitor targeting cyclin-dependent kinase 4/9 (CDK4/9) and histone deacetylase1 (HDAC1) against malignant cancer, *J. Med. Chem.* 61(2018), 3166–3192.
- [25] D. Rudolph, M. Steegmaier, M. Hoffmann, M. Grauert, A. Baum, J. Quant, C. Haslinger, P. Garin-Chesa, G.R. Adolf, BI 6727, a Polo-like Kinase inhibitor with improved pharmacokinetic profile and broad antitumor activity, *Clin. Cancer Res.* 15 (2009) 3094–3102.
- [26] K. Ko, H.J. Kim, P.S. Ho, S.O. Lee, J.E. Lee, C.R. Min, Y.C. Kim, J.H. Yoon, E.J. Park, Y.J.

Kwon, J.H. Yun, D.O. Yoon, J.S. Kim, W.S. Park, S.S. Oh, Y.M. Song, W.K. Cho, K. Morikawa, K.J. Lee, C.H. Park, Discovery of a novel highly selective histamine H4 receptor antagonist for the treatment of atopic dermatitis, *J. Med. Chem.* 61(2018) 2949-2961.

[27] E.J. Barreiro, A.E. Kümmerle, C.A.M. Fraga, The methylation effect in medicinal chemistry, *Chem. Rev.* 111 (2011) 5215–5246.

[28] C.A. Lipinski, F. Lombardo, B.W. Dominy, P.J. Feeney, Experimental and computational approaches to estimate solubility and permeability in drug discovery and development settings, *Adv. Drug Deliv. Rev.* 23 (1997) 3–25.

[29] D.F. Veber, S.R. Johnson, H.Y. Cheng, B.R. Smith, K.W. Ward, K.D. Kopple, Molecular properties that influence the oral bioavailability of drug candidates, *J. Med. Chem.* 45 (2002) 2615–2623.

[30] N.A. Meanwell, Improving drug candidates by design: a focus on physicochemical properties as a means of improving compound disposition and safety, *Chem. Res. Toxicol.* 24 (2011) 1420–1456.

[31] de Santana TI, Barbosa MO, Gomes PATM, da Cruz ACN, da Silva TG, Leite ACL, Synthesis, anticancer activity and mechanism of action of new thiazole derivatives, *Eur. J. Med. Chem.* 144 (2018) 874–886.

[32] A. Daina, O. Michielin, V. Zoete, SwissADME: a free web tool to evaluate pharmacokinetics, drug-likeness and medicinal chemistry friendliness of small molecules, *Sci. Rep.* 7 (2017) 42717.

[33] Y.H. Chu, Y.Li, Y.T. Wang, B. li, Y.H. Zhang, Investigation of interaction modes involved in alkaline phosphatase and organophosphorus pesticides *via* molecular simulations, *Food Chem.* 254 (2018) 80–86.

Highlights

1. Two series of novel pteridinone derivatives were designed and synthesized in this study.
2. *In vitro* antiproliferative activity screening and SARs study for all the targeted compounds.
3. The PLK1 was likely to be one of the drug targets of compound **L**₇.
4. Compound **L**₇ could induce apoptosis by the wound-healing and AO/EB assays.
5. Compound **L**₇ effectively arrested A549 cells in G1 stage through flow cytometry.